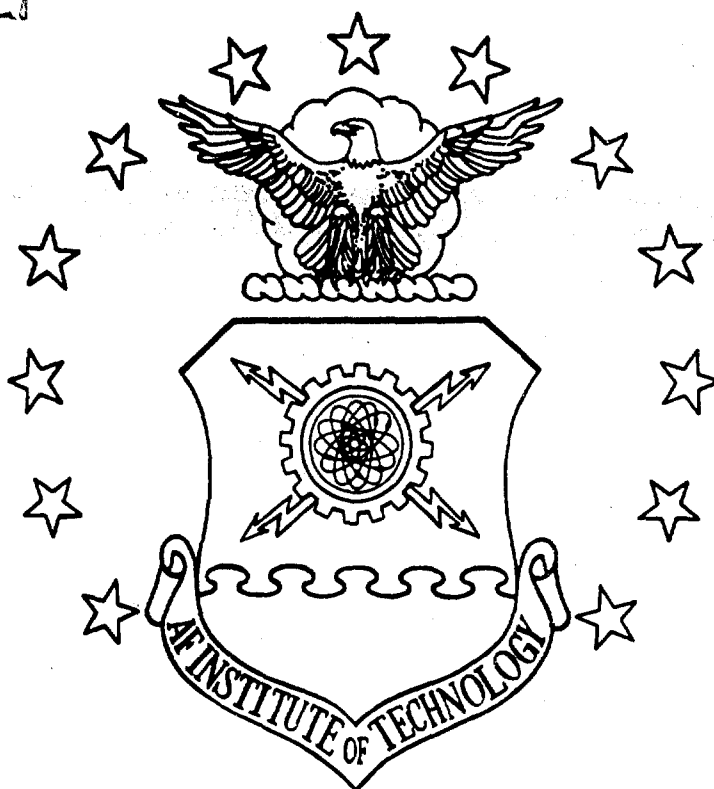


DWG FILE COPY

AD-A230 441



DTIC
ELECTE
JAN 03 1991
S E D

DEPARTMENT OF THE AIR FORCE
AIR UNIVERSITY

AIR FORCE INSTITUTE OF TECHNOLOGY

Wright-Patterson Air Force Base, Ohio

31 1 3 072

DISTRIBUTION STATEMENT A

Approved for public release;
Distribution Unlimited

AFIT/GE/ENG/90D-53

THE RADAR RANGE EQUATION
FOR THE DETECTION OF STEADY
TARGETS IN WEIBULL CLUTTER

THESIS

Leon C. Rountree

AFIT/GE/ENG/90D-53

SD DTIC
ELECTE
JAN 08 1991
E D

Approved for public release; distribution unlimited

AFIT/GE/ENG/90D-53

THE RADAR RANGE EQUATION FOR THE DETECTION
OF STEADY TARGETS IN WEIBULL CLUTTER

THESIS

Presented to the Faculty of the School of Engineering
of the Air Force Institute of Technology

Air University

In Partial Fulfillment of the
Requirements for the Degree of
Master of Science in Electrical Engineering

Leon C. Rountree, B.S., B.E.E.

December 1990

Accession For	
NTIS	GRA&I <input checked="" type="checkbox"/>
DTIC	TAB <input checked="" type="checkbox"/>
Unannounced	<input type="checkbox"/>
Justification	
By _____	
Distribution/	
Availability Codes	
Dist	Avail and/or Special
A-1	

Approved for public release; distribution unlimited



Preface

The purpose of this study was to develop the detection characteristics of a steady target in Weibull radar clutter and to provide a means of predicting the radar detection range of such targets. This problem originated after first investigating the problem of predicting the radar detection range of helicopters flying nap of the earth profiles. This study can be considered as a first step in the approach to such a problem.

I became interested in radar detection problems through my courses at AFIT and chose this particular research project after being introduced to it by my thesis advisor.

I wish to express my gratitude to everyone who helped me to complete this thesis. I thank my thesis advisor, Dr. Vittal Pyati, for introducing me to this topic and for the guidance he provided through the course of my research. I am also grateful to the members of my thesis committee, Lt. Col. David Meer, Lt. Col. Dave Norman, and Dr. B.N. Nagarsenker, for their comments and suggestions. I also wish to thank my classmates in GE-90D and especially those in the Communications-Radar section for their help with this thesis effort as well as our course work. Finally, I want to extend a special thanks to my wife, Kathy, for the encouragement, support, and love that she provided throughout this project.

Leon C. Rountree

Table of Contents

	Page
Preface	ii
Table of Contents	iii
List of Figures	v
List of Tables	vii
Abstract	viii
 I. Introduction	 1
1.1 Application	1
1.2 Problem Statement	2
1.3 Scope	2
1.4 Assumptions	2
1.5 General Approach	3
1.6 Sequence of Presentation	3
1.7 Equipment	4
 II. Background	 5
2.1 Target Detection in Gaussian Noise	5
2.2 Weibull Clutter Model	5
2.2.1 Justification for the Weibull Model.	5
2.2.2 Weibull Parameters for Clutter Distributions. . .	6
2.3 Detection in Weibull Clutter	7

	Page
III. Development of Detection Characteristics	9
3.1 Rayleigh-to-Weibull Transformation	9
3.2 Detector Model	10
3.3 Radar Parameter Calculations	12
3.3.1 Probability of False Alarm.	12
3.3.2 Probability of Detection.	13
3.4 Relationship between SCR, P_{fa} , and P_d	15
3.5 Radar Range Equation	17
IV. Computer Implementation	20
4.1 Algorithm to Compute Q function	20
4.2 Computational Problems	21
4.3 Computer Program Design	23
4.4 Results	53
4.4.1 Validation.	53
4.4.2 Comparison of Results for Various Values of b. . .	53
V. Conclusions and Recommendations	55
5.1 Conclusions	55
5.2 Recommendations for Future Research	55
5.2.1 Weibull Target.	55
5.2.2 Other Recommendations.	58
5.3 Summary	58
Appendix A. Computer Program Listing	59
Appendix B. Weibull Probability Density Function	65
Bibliography	66
Vita	68

List of Figures

Figure	Page
1. Detector for Deterministic Signal in Gaussian Noise	10
2. Detector Model for Deterministic Signal in Weibull Clutter	11
3. Program Flowchart	25
4. P_d versus SCR for $b = 2$	26
5. P_d versus SCR for $b = 1.8$	27
6. P_d versus SCR for $b = 1.6$	28
7. P_d versus SCR for $b = 1.4$	29
8. P_d versus SCR for $b = 1.2$	30
9. P_d versus SCR for $b = 1$	31
10. P_d versus SCR for $b = .8$	32
11. P_d versus SCR for $b = .6$	33
12. P_d versus SCR for $b = .5$	34
13. P_d versus R/R_o for $b = 2$ and large grazing angles	35
14. P_d versus R/R_o for $b = 1.8$ and large grazing angles	36
15. P_d versus R/R_o for $b = 1.6$ and large grazing angles	37
16. P_d versus R/R_o for $b = 1.4$ and large grazing angles	38
17. P_d versus R/R_o for $b = 1.2$ and large grazing angles	39
18. P_d versus R/R_o for $b = 1$ and large grazing angles	40
19. P_d versus R/R_o for $b = .8$ and large grazing angles	41
20. P_d versus R/R_o for $b = .6$ and large grazing angles	42
21. P_d versus R/R_o for $b = .5$ and large grazing angles	43
22. P_d versus R/R_o for $b = 2$ and small grazing angles	44
23. P_d versus R/R_o for $b = 1.8$ and small grazing angles	45
24. P_d versus R/R_o for $b = 1.6$ and small grazing angles	46

Figure	Page
25. P_d versus R/R_o for $b = 1.4$ and small grazing angles	47
26. P_d versus R/R_o for $b = 1.2$ and small grazing angles	48
27. P_d versus R/R_o for $b = 1$ and small grazing angles	49
28. P_d versus R/R_o for $b = .8$ and small grazing angles	50
29. P_d versus R/R_o for $b = .6$ and small grazing angles	51
30. P_d versus R/R_o for $b = .5$ and small grazing angles	52
31. Weibull pdf	65

List of Tables

Table	Page
1. Weibull Skewness Parameter for Clutter Returns	7
2. Additional SCR and Decrease in Detection Range	54

Abstract

In this thesis, the detection characteristics of a steady target immersed in radar clutter characterized by returns statistically modeled according to a Weibull probability density function are developed. A detector model is developed which is a modification of an envelope detection scheme used to detect deterministic signals in Gaussian noise. By examining the statistics of the output of the detector under alternate hypotheses, an expression for the probability of detection (P_d) is developed in terms of the probability of false alarm (P_{fa}), the signal-to-clutter ratio (SCR), and the Weibull skewness parameter (b), which is a function of the type of terrain causing the clutter. This expression is used in conjunction with a form of the radar range equation for area clutter to produce equations which describe the relationship between P_d , P_{fa} , SCR, b , and the radar detection range. These equations involve Marcum's Q function and an algorithm is presented which evaluates this function. The algorithm is a series approximation and can be computed to a desired accuracy. The algorithm is also presented as a recursive relationship and it is implemented using a FORTRAN computer program. Plots of P_d versus SCR and P_d versus range are developed for various values of P_{fa} and b . The plots provide a means of evaluating the detector performance and predicting the detection range for several values of b ; thus for several types of terrain.

THE RADAR RANGE EQUATION FOR THE DETECTION OF STEADY TARGETS IN WEIBULL CLUTTER

I. Introduction

The practical problem of predicting the radar detection range of targets in radar clutter requires a modification to the standard radar range equation found in textbooks and other literature. The standard radar range equation is derived under the assumption that the primary factor limiting detectability is noise created within the receiver and captured by the antenna. This assumption is inadequate for targets in radar clutter because detectability is not limited by noise alone. It is limited by clutter returns caused by trees and terrain, which in most cases overwhelms receiver noise.

Receiver and antenna noise voltage amplitude is typically modeled as a Gaussian random process and the problem of the detection of a steady target, or a target characterized by a deterministic signal, in Gaussian noise is well-documented. However, the detection problem of targets in non-Gaussian interference is the topic of recent research. To accurately predict the radar detection range of steady targets in radar clutter, a statistical model of the clutter must be developed. Recent literature suggests that the Weibull probability density function (pdf) can be used to model the nature of radar returns from land and sea clutter (1:1) (6:221) (3:736).

1.1 Application

The prediction of the radar detection range of targets in radar clutter can be applied to the problem of determining the radar detection range of helicopters flying nap of the earth (NOE) profiles. Helicopters pilots use NOE flight to avoid radar

detection. The helicopter target signal becomes immersed in the clutter returns caused by the terrain when the helicopter flies close to the ground. The problem of detecting steady targets in Weibull clutter can be used as a first step in the analysis of the problem of detection of helicopters flying NOE profiles.

1.2 Problem Statement

This thesis addresses the problem of predicting the radar detection range of steady targets immersed in radar clutter characterized by returns that can be statistically modeled according to a Weibull pdf.

1.3 Scope

The detection characteristics of a deterministic, or exactly known, signal corrupted by clutter interference modeled according to a Weibull pdf will be developed. The objectives of this thesis are to determine the relationship between the probability of detection, the probability of false alarm, and the signal-to-clutter ratio (SCR) for deterministic signals detected in Weibull clutter and to develop a set of curves that shows the minimum required SCR and the maximum detection range for a desired probability of detection for various values of probability of false alarm.

The curves will be developed for different values of the skewness parameter, b , of the Weibull pdf (see Appendix B). Different values of b have been found to correspond to different types of terrain when the radar returns from the terrain are statistically modeled according to a Weibull pdf (18:737-738). The values of b used to develop these curves will span the range of typical values representing several types of terrain.

1.4 Assumptions

The primary assumption made is that the target to be detected is a steady target. That is, the amplitude of the return signal from the target is exactly known.

Also, the detection of the target will be carried out with a single pulse observation of the target's return signal.

The radar clutter will be assumed to be area clutter spread over a patch of terrain. It will also be assumed that the interference caused by the radar clutter will overwhelm the receiver and antenna noise so that the noise can be considered negligible leaving the clutter as the only interference corrupting the signal.

1.5 General Approach

The first step in the approach to this problem is to develop a detector model that simulates a detection scheme for steady targets in Weibull clutter. This model can be developed by modifying a detection scheme commonly used to detect steady targets in Gaussian noise.

By examining the statistics of the output of the detector model under the hypotheses of a signal present and clutter alone present, expressions for the probability of detection, P_d , and the probability of false alarm, P_{fa} , can be found for the detection of steady targets in Weibull clutter. These expressions describe the relationship between the P_d , the P_{fa} , and the signal-to-clutter ratio, SCR.

This relationship can be applied to a modified form of the radar range equation for area clutter to determine the relationship between the maximum radar detection range, P_d , and P_{fa} . Finally, the mathematical expressions that describe these relationships are examined using digital computation in order to develop plots of P_d versus SCR and P_d versus range for different values of P_{fa} and Weibull skewness parameters.

1.6 Sequence of Presentation

First a summary of how the Weibull pdf can be used to model radar surface clutter is presented in Chapter 2. Chapter 2 also includes a presentation of analyses of the detection problem of steady targets in Weibull interference.

The expressions relating P_d , P_{fa} , SCR, and range are developed in Chapter 3. Chapter 4 contains the evaluation of these expression using a FORTRAN computer program. Plots displaying the relationship between P_d , P_{fa} , SCR, and range are also included in Chapter 4.

Finally, conclusions are presented and recommendations for further research are suggested in Chapter 5. An introduction to the problem of detecting a Weibull target in Weibull clutter is included in the recommendations. A listing of the computer program used to develop the plots described above is included as an appendix.

1.7 Equipment

A VAX 11/785 computer with a FORTRAN 77 compiler is used to implement the computer program found in Appendix A.

II. Background

In this chapter, the Weibull clutter model is introduced and some existing analyses of steady target detection in Weibull clutter is reviewed. First, the detection problem of a deterministic signal in Gaussian noise is recalled.

2.1 Target Detection in Gaussian Noise

Marcum and Swerling produced a definitive study of the statistical problem of target detection by a pulse radar. Marcum's paper dealt with steady target detection in Gaussian noise, while Swerling extended Marcum's results to the case of fluctuating targets in Gaussian noise. Swerling created four statistical models for different types of fluctuating targets which are commonly referred to in radar literature as Cases 1, 2, 3, and 4. Marcum's work has become known as Case 0 (12:62-83,273-288). Marcum's Case 0 will be the problem examined in this thesis with the exception of the signal interference no longer being Gaussian noise but Weibull clutter.

Marcum created expressions for P_d and P_{fa} for Case 0. He also determined the relationship between P_d , P_{fa} , and the maximum detection range and plotted the results (12:85-138). Marcum's expression for P_d has become known as Marcum's Q function (14:40). The Q function will be discussed more in Chapters 3 and 4.

2.2 Weibull Clutter Model

2.2.1 Justification for the Weibull Model. Several pdfs have been used to model the nature of radar signal returns from land and sea clutter. Both log-normal and Rayleigh pdfs have been used to model clutter statistically in terms of spatial distribution. The Rayleigh pdf has been used for clutter observed at large grazing angles (greater than 5 degrees). The log-normal distribution has been used more for

small grazing angles because at small angles, land clutter density generally varies over a wider range than the Rayleigh pdf is suited for (1:1).

In Schleher's paper, he states that the Rayleigh model usually underestimates the dynamic range of the clutter distribution, while the log-normal model overestimates it. The Weibull pdf can be made to approach either the Rayleigh or the log-normal by an adjustment of its parameters and it can be used as a model over a wider range of conditions. Schleher further states:

From a detection standpoint, it can be said that the log-normal distribution represents the worst case distribution, the Rayleigh the best case, and the Weibull an intermediate model that may more accurately represent the real detection performance in clutter. (18:736-737)

The Weibull pdf has been found to correspond to some land clutter distributions quite well. There are several sources of measured distributions of clutter that exhibit a Weibull distribution. Data have been recorded for several types of terrain including grasslands, forests, cultivated land, and mountains. All these cases were found to fit the Weibull pdf (1:1-12). Data taken from radars illuminating the ocean indicate that sea clutter is also distributed according to a Weibull pdf (3:929).

2.2.2 Weibull Parameters for Clutter Distributions. A graphical technique for determining if measured distributions of clutter returns can be represented by a Weibull pdf is available. The equation describing the Weibull distribution can be manipulated so that the variate of the distribution is expressed as a linear function of the median of the distribution and the Weibull skewness parameter, b . The slope of the line created by this function is equal to $1/b$. Measured clutter distributions can be plotted to determine if the distribution fits the Weibull model and to determine the value of b . If the points lie in a reasonably straight line, the Weibull distribution can be used to model the clutter (1:2-4).

Table 1. Weibull Skewness Parameter for Clutter Returns (15:234)

Terrain/Sea state	Freq	Beam-width($^{\circ}$)	Grazing angle($^{\circ}$)	Pulse-length(μ s)	b
Rocky mountains	S	1.5	-	2	.512
Wooded hills	L	1.7	.5	3	.626
Forest	X	1.4	.7	.17	.506-.513
Cultivated land	X	1.4	.7-5	.17	.606-2
Sea state 1	X	.5	4.7	.02	1.452
Sea state 2	K_u	5	1-30	.1	1.16-1.783

Several measured distributions of clutter returns from various terrain types which exhibit the Weibull distribution have been obtained. Table 1 shows the values of b which correspond to different types of land and sea clutter (15:233-234).

2.3 Detection in Weibull Clutter

An approximate analysis of the detection characteristics for a steady target in Weibull clutter was made by Ekstrom. In this analysis, it was assumed that the signal voltage was much greater than the median voltage value of the clutter return distribution. Under this assumption, closed form expressions that approximate the P_d when P_d is greater than 1/2 were developed (6:222-225).

Schleher has examined the problem more thoroughly by using the Weibull and the Weibull-Ricean pdfs to describe the statistics of the output of an envelope detector receiver under the hypotheses of clutter alone present and signal plus clutter present respectively. Although the details of the analysis are not included in his report, the P_d was determined "using a characteristic function approach in conjunction with the fast-Fourier transform." The results of this study are plots of P_d versus signal-to-clutter ratio for a P_{fa} of 10^{-6} and b equal to 2, 1.2, .8, and .6 (18:737-739). These plots can be compared to the ones developed in this thesis.

Other researchers have taken the problem a step further by allowing the target

to be a fluctuating one. Goldstein obtained expressions for the P_d of a Rayleigh target in Weibull clutter. These results are based on the assumption that the signal-to-clutter ratio is large. For fluctuating targets, the pdf of the envelope of the received signal when both target and clutter are present can be approximated by the pdf of the target signal's envelope when the signal-to-clutter ratio is large (9:90-91). Chen and Morchin also used this fact in developing an expression for P_d of a Rayleigh target in Weibull clutter. Their results were plotted for b equal to .5, .6, .7, and .8 (3:929-932).

III. Development of Detection Characteristics

The problem of detecting a signal known exactly corrupted by Weibull clutter interference can be approached by first examining the detection problem of a deterministic signal immersed in Gaussian noise. When white Gaussian noise alone is passed through a narrowband filter, the probability density function (pdf) of the envelope of the output noise voltage is Rayleigh. The envelope of Gaussian noise plus a deterministic signal passed through a narrowband filter is distributed according to a Ricean pdf (19:23-27). These results will be useful in the analysis of the detection problem in Weibull clutter.

3.1 Rayleigh-to-Weibull Transformation

A Rayleigh random variable, r , representing the envelope of a narrowband Gaussian process can be transformed into a Weibull random variable, w , by raising r to a power, ν (8:10-11):

$$w = |r^\nu| \quad (1)$$

The value of ν that will result in w being a Weibull random variable is found by performing the transformation of equation 1 on r . The variable, r , has a Rayleigh pdf as shown:

$$p(r) = (r/\sigma^2) \exp(-r^2/2\sigma^2) \quad r > 0 \quad (2)$$

The parameter, σ^2 , is the mean-square voltage of the Gaussian input. The pdf of w is found as follows

$$\begin{aligned} p(w) &= p(r = w^{1/\nu}) |dr/dw| \\ &= (w^{(2/\nu-1)}/\nu\sigma^2) \exp(-w^{2/\nu}/2\sigma^2) \quad w > 0 \end{aligned} \quad (3)$$

A Weibull pdf has the form

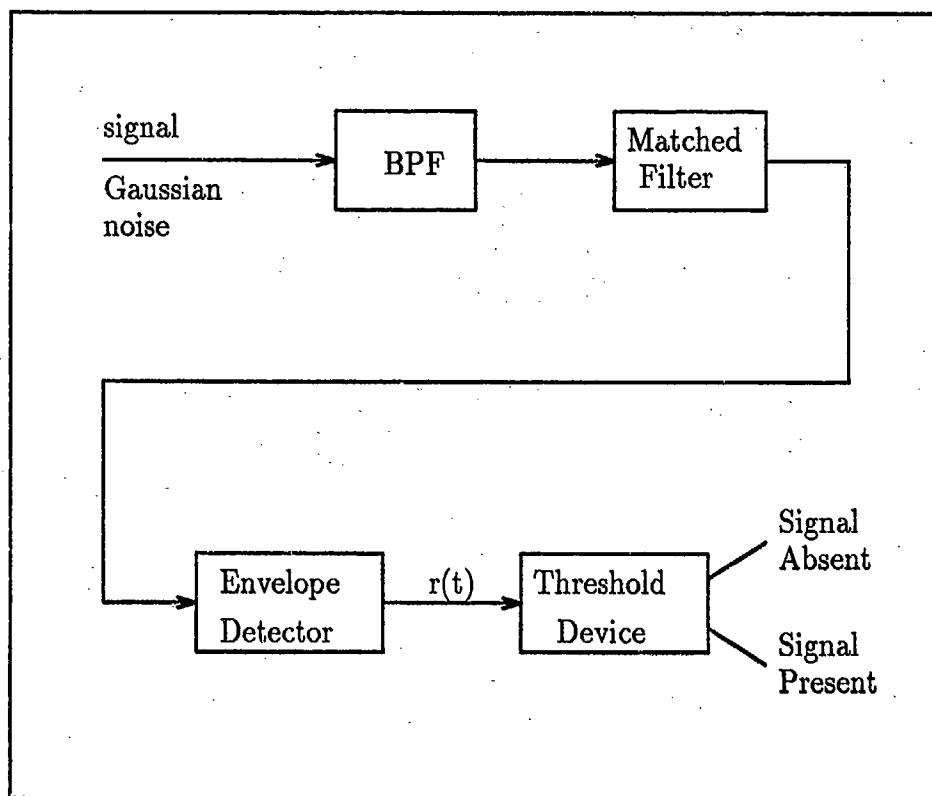


Figure 1. Detector for Deterministic Signal in Gaussian Noise

$$p(x) = (b/\alpha)x^{b-1} \exp(-x^b/\alpha) \quad x > 0 \quad (4)$$

From equations 3 and 4, it can be seen that w is Weibull when

$$\nu = 2/b \quad (5)$$

3.2 Detector Model

The Weibull envelope clutter process can be modeled artificially by modifying a detection scheme used to detect a signal known exactly with unknown phase in Gaussian noise. A simplified block diagram of a detector to detect exactly known signals with unknown phase in Gaussian noise is shown in Figure 1 (5:298-302).

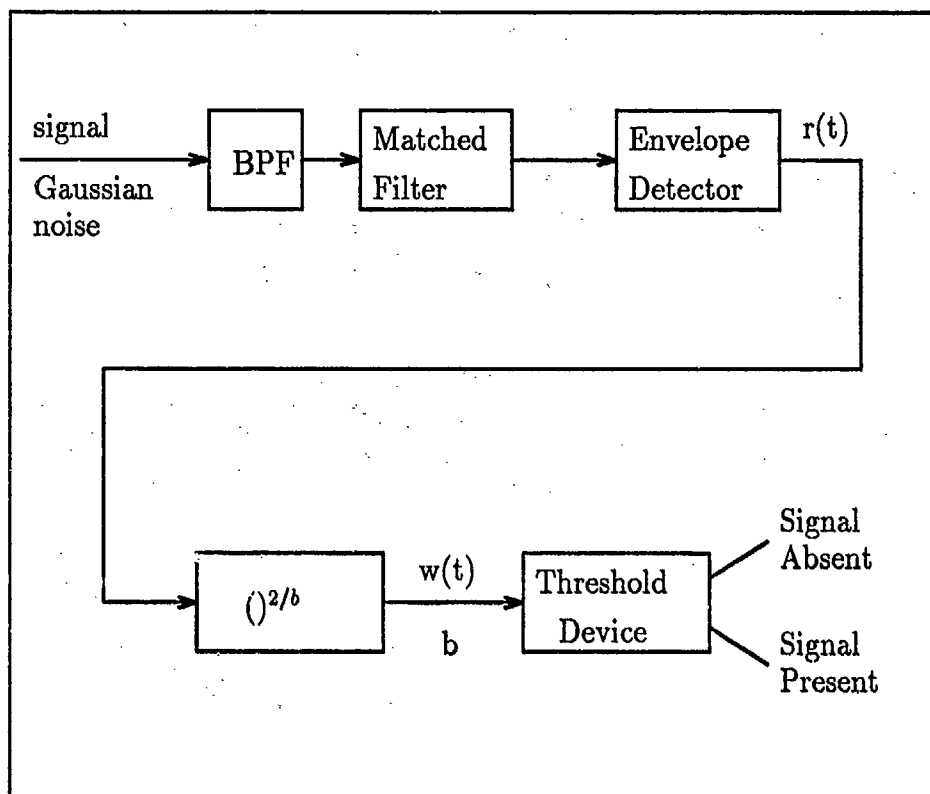


Figure 2. Detector Model for Deterministic Signal in Weibull Clutter

Using the results of the previous section, it is seen that a Weibull process can be simulated by introducing an operation after the envelope detector that will transform the the Rayleigh variable, r , into a Weibull variable, w , when noise alone is present. The operation necessary is determined from equations 1 and 5 and is given by

$$w = r^{(2/b)} \quad (6)$$

A block diagram for this detector is shown in Figure 2.

Use of this model allows one to approach the detection problem of a deterministic signal in Weibull clutter by first taking advantage of the well-documented results of the detection of a deterministic signal in Gaussian noise.

3.3 Radar Parameter Calculations

3.3.1 Probability of False Alarm. When there is no target signal present, the signals, $r(t)$ and $w(t)$, from Figure 2 are distributed according to Rayleigh and Weibull pdfs respectively. The pdf of $w(t)$ is

$$p(w/H_o) = (b/\alpha)w^{b-1} \exp(-w^b/\alpha) \quad w > 0 \quad (7)$$

where H_o represents the hypothesis that no target is present. The parameter, b , indicates the degree of skewness in the distribution and α is related to the median of the distribution (15:234). While b is determined by the type of terrain causing the clutter returns, α is determined by the mean-square voltage, σ^2 , of the Gaussian input. It can be seen from equations 3 and 4 that $\alpha = 2\sigma^2$. The parameter, α , is related to the median by (1:2)

$$w_m = (\alpha \ln(2))^{1/b} \quad (8)$$

where w_m is the median. From equation 8 and the relation that $\alpha = 2\sigma^2$, it is seen that

$$\sigma^2 = w_m^b / (2 \ln(2)) \quad (9)$$

The probability of false alarm is determined by integrating the pdf of equation 7 from the detection threshold, w_T , to infinity:

$$\begin{aligned} P_{fa} &= \int_{w_T}^{\infty} (b/\alpha)w^{b-1} \exp(-w^b/\alpha)dw \\ &= \exp(-w_T^b/2) \end{aligned} \quad (10)$$

When P_{fa} is a fixed parameter, w_T can be solved for:

$$w_T = (2 \ln(1/P_{fa}))^{1/b} \quad (11)$$

3.3.2 *Probability of Detection.* When an exactly known signal is present at the input of the detector, $r(t)$ has a Ricean pdf. Using DiFranco and Rubin's notation, the Ricean pdf is

$$p(r/H_1) = r \exp[-(r^2 + \mathcal{R})/2] I_0(r\sqrt{\mathcal{R}}) \quad r > 0 \quad (12)$$

where H_1 is the hypothesis that a signal is present and $I_0()$ represents the zero-order modified Bessel function of the first kind. \mathcal{R} is defined to be $2E/N_0$ where E is the detected target signal energy and N_0 is the one-sided power spectral density of a zero-mean white Gaussian noise input. DiFranco and Rubin refer to the parameter, \mathcal{R} , as the peak signal-to-noise power ratio, which is the ratio of maximum instantaneous signal power to average noise power out of a matched filter. \mathcal{R} appears often in radar literature (5:302-307).

When a signal is present, $r(t)$ undergoes the transformation of equation 6 and $w(t)$ has the pdf developed below:

$$\begin{aligned} p(w/H_1) &= p(r = w^{1/\nu}) | dr/dw | \\ &= w^{1/\nu} \exp[-(w^{2/\nu} + \mathcal{R})/2] I_0(w^{1/\nu} \sqrt{\mathcal{R}}) (1/\nu) w^{(1/\nu)-1} \\ &= (w^{(2/\nu)-1}/\nu) \exp[-(w^{2/\nu} + \mathcal{R})/2] I_0(w^{1/\nu} \sqrt{\mathcal{R}}) \quad w > 0 \end{aligned} \quad (13)$$

Substituting $\nu = 2/b$, $p(w/H_1)$ becomes

$$p(w/H_1) = (b/2) w^{b-1} \exp[-(w^b + \mathcal{R})/2] I_0(w^{b/2} \sqrt{\mathcal{R}}) \quad w > 0 \quad (14)$$

To determine the probability of detection for a signal known exactly in Weibull envelope clutter, equation 14 is integrated from the detection threshold, w_T , to infinity:

$$P_d = \int_{w_T}^{\infty} (b/2) w^{b-1} \exp[-(w^b + \mathcal{R})/2] I_0(w^{b/2} \sqrt{\mathcal{R}}) dw \quad (15)$$

This equation is of the form of Marcum's Q function given by (14:40)

$$Q(\alpha, \beta) = \int_{\beta}^{\infty} v \exp[-(v^2 + \alpha^2)/2] I_0(\alpha v) dv \quad (16)$$

Making the following substitutions:

$$\alpha = \sqrt{\mathcal{R}}$$

$$\beta = w_T$$

$$v = w^{b/2}$$

$$dv = (b/2)w^{(b/2)-1}dw$$

the integral of equation 15 can be written as

$$P_d = \int_{w_T}^{\infty} v \exp[-(v^2 + \mathcal{R})/2] I_0(v\sqrt{\mathcal{R}}) dv \quad (17)$$

$$= Q(\sqrt{\mathcal{R}}, w_T) \quad (18)$$

Combining equations 11 and 18, P_d becomes

$$P_d = Q(\sqrt{\mathcal{R}}, (2 \ln(1/P_{fa}))^{1/b}) \quad (19)$$

Also, Marcum's Q function can be written in terms of the incomplete Toronto function as (12:160)

$$Q(\alpha, \beta) = 1 - T_{\beta/\sqrt{2}}(1, 0, \alpha/\sqrt{2}) \quad (20)$$

Therefore, P_d becomes

$$P_d = 1 - T_{(2 \ln(1/P_{fa}))^{1/b}/\sqrt{2}}(1, 0, (\mathcal{R}/2)^{1/2}) \quad (21)$$

When $b = 2$, it is seen that the pdf of $w(t)$ is Rayleigh and the P_d and P_{fa} are the same as those found for the case of an exactly known signal with unknown phase

detected in the presence of Gaussian noise with an envelope detector. Several texts, including DiFranco and Rubin's contain plots that show the required peak signal-to-noise ratio, \mathcal{R} , needed to achieve a desired probability of detection for various values of false alarm (5:308). These plots are identical to the ones that would be created by an evaluation of equation 19 with $b = 2$.

3.4 Relationship between SCR, P_{fa} , and P_d

In the case of the detection of a deterministic signal corrupted by Weibull clutter, b is typically not equal to 2 and P_d is determined by equation 19 or 21. When the target signal is corrupted by Weibull clutter, it is more meaningful to use a signal-to-clutter ratio (SCR), instead of the parameter, \mathcal{R} .

The clutter power is determined from the second moment of the Weibull pdf of equation 7 as (15:34)

$$E[w^2] = \Gamma(1 + (2/b)) \frac{w_m^2}{(\ln(2))^{2/b}} \quad (22)$$

where $\Gamma()$ is the Gamma function and w_m is the median of the Weibull distribution. If the amplitude of the signal before the envelope detector is A , the power signal-to-clutter ratio at point b of Figure 2 is

$$\begin{aligned} SCR_b &= \frac{(A^{2/b})^2}{(w_m^2 / (\ln 2)^{2/b}) \Gamma(1 + (2/b))} \\ &= \frac{(A^2)^{2/b} (\ln 2)^{2/b}}{w_m^2 \Gamma(1 + (2/b))} \end{aligned} \quad (23)$$

Recall that \mathcal{R} is the peak signal-to-noise power ratio. The peak signal power is related to the average instantaneous power by (5:296)

$$(\text{peak instantaneous signal power}) = 2(\text{average instantaneous signal power}) \quad (24)$$

The average instantaneous signal power of a sinusoidal signal of amplitude, A , is $A^2/2$ and the average noise power is σ^2 . Therefore, \mathcal{R} expressed in terms of σ^2 is

$$\begin{aligned}\mathcal{R} &= [2(A^2/2)]/\sigma^2 \\ &= A^2/\sigma^2\end{aligned}\tag{25}$$

Using equation 9, it is seen that

$$\mathcal{R} = (A^2 2 \ln 2)/w_m^b\tag{26}$$

Therefore, SCR_b is related to \mathcal{R} by

$$SCR_b = \frac{(\mathcal{R}/2)^{2/b}}{\Gamma(1 + (2/b))}\tag{27}$$

To determine the SCR at the input of the envelope detector, the inverse of the transformation of equation 6 can be performed on SCR_b to give

$$\begin{aligned}SCR &= (SCR_b)^{b/2} \\ &= \frac{\mathcal{R}}{2[\Gamma(1 + (2/b))]^{b/2}}\end{aligned}\tag{28}$$

This leads to

$$\mathcal{R} = 2(SCR)[\Gamma(1 + (2/b))]^{b/2}\tag{29}$$

$$\sqrt{\mathcal{R}} = [2(SCR)]^{1/2}[\Gamma(1 + (2/b))]^{b/4}\tag{30}$$

Combining equations 18 and 30, the relationship between SCR, P_{fa} , and P_d is

$$P_d = Q([2(SCR)]^{1/2}[\Gamma(1 + (2/b))]^{b/4}, [2 \ln(1/P_{fa})]^{1/b})\tag{31}$$

where $Q(\alpha, \beta)$ is Marcum's Q function.

3.5 Radar Range Equation

The radar range equation for targets in area clutter can be divided into two cases: beamwidth-limited case and pulse-length-limited case. For large grazing angles, the area of terrain illuminated by the radar is limited by antenna beamwidth; while for small grazing angles, the area is limited by the pulse-length of the transmitted signal. The radar range equations for each of these two cases are (16:63-67)

$$R^2 = \frac{L(\sin \psi)\sigma_t}{(\pi/4)\theta\phi(SCR)\sigma_o} \quad \text{for} \quad \tan \psi > \frac{\phi R}{c\tau/2} \quad (32)$$

and

$$R = \frac{L(\cos \psi)\sigma_t}{(SCR)(c\tau/2)\theta\sigma_o} \quad \text{for} \quad \tan \psi < \frac{\phi R}{c\tau/2} \quad (33)$$

where

- L = all of the various losses encountered by the radar
- ψ = grazing angle of the radar
- σ_t = target radar cross section
- SCR = mean signal-to-clutter power ratio
- σ_o = the backscatter (clutter) radar cross section per unit area of reflecting surface (m^2/m^2)
- θ = 3-dB beamwidth in azimuth
- ϕ = 3-dB beamwidth in elevation
- τ = pulse duration of the transmitted signal
- c = speed of light
- R = radar detection range

The SCR can be solved for to obtain

$$SCR = \frac{L(\sin \psi)\sigma_t}{R^2(\pi/4)\theta\phi\sigma_o} \quad \text{for} \quad \tan \psi > \frac{\phi R}{c\tau/2} \quad (34)$$

and

$$SCR = \frac{L(\cos \psi)\sigma_t}{R(c\tau/2)\theta\sigma_o} \quad \text{for} \quad \tan \psi < \frac{\phi R}{c\tau/2} \quad (35)$$

Now, define a normalizing range, R_o , which is the range at which the SCR becomes unity (2:23-27). Using equations 34 and 35, R_o becomes

$$R_o = \left(\frac{L(\sin \psi)\sigma_t}{(\pi/4)\theta\phi\sigma_o} \right)^{1/2} \quad \text{for} \quad \tan \psi > \frac{\phi R}{c\tau/2} \quad (36)$$

and

$$R_o = \frac{L(\cos \psi)\sigma_t}{(c\tau/2)\theta\sigma_o} \quad \text{for} \quad \tan \psi < \frac{\phi R}{c\tau/2} \quad (37)$$

Now, all radar parameters are included in R_o and SCR can be related to range readily by

$$R/R_o = (1/SCR)^{1/2} \quad \text{for} \quad \tan \psi > \frac{\phi R}{c\tau/2} \quad (38)$$

and

$$R/R_o = 1/SCR \quad \text{for} \quad \tan \psi < \frac{\phi R}{c\tau/2} \quad (39)$$

Therefore, for small grazing angles (pulse-length-limited case), the detection range is inversely proportional to the SCR. For larger grazing angles (beamwidth-limited case), the detection range is inversely proportional to the square root of the SCR.

The relationship between detection range, P_d , and P_{fa} can be determined by combining equations 31, 38, and 39:

$$P_d = Q(\sqrt{2}(R_o/R)[\Gamma(1 + (2/b))]^{b/4}, [2 \ln(1/P_{fa})]^{1/b}) \quad \text{for} \quad \tan \psi > \frac{\phi R}{c\tau/2} \quad (40)$$

where

$$R_o = \left(\frac{L(\sin \psi)\sigma_t}{(\pi/4)\theta\phi\sigma_o} \right)^{1/2} \quad (41)$$

and

$$P_d = Q((2R_o/R)^{1/2}[\Gamma(1 + (2/b))]^{b/4}, [2\ln(1/P_{fa})]^{1/b}) \text{ for } \tan \psi < \frac{\phi R}{c\tau/2} \quad (42)$$

where

$$R_o = \frac{L(\cos \psi)\sigma_t}{(c\tau/2)\theta\sigma_o} \quad (43)$$

Equations 40 and 42 along with equation 31 can be evaluated to obtain plots of P_d versus R/R_o and P_d versus SCR for various values of P_{fa} and b . The detection problem becomes a problem of evaluating the Q function for the arguments shown in equations 31, 40, and 42. This is the subject of Chapter 4.

IV. Computer Implementation

The expressions for P_d from equations 31, 40, and 42 describe the detection characteristics of a steady target in Weibull clutter. In order to evaluate these expressions, a means of tabulating Marcum's Q function must be developed.

4.1 Algorithm to Compute Q function

In a Johns Hopkins University report by Fehlner, an algorithm for computing Marcum's Q function was developed. The integrand of the Q function was re-derived using the characteristic function and the Q function was finally expressed as a series (7:23).

The characteristic function for Marcum's Case 0 is the Fourier transform of the integrand of the Q function of equation 16. First, the substitution, $u = v^2/2$ and $du = vdu$ is made to obtain the integrand, I:

$$I = \exp[-(u + \alpha^2/2)] I_0(\alpha\sqrt{2u}) \quad u > 0 \quad (44)$$

The characteristic function becomes

$$C = \int_0^\infty \exp[-(u + \alpha^2/2)] I_0(\alpha\sqrt{2u}) e^{j\omega u} du \quad (45)$$

Letting $x = \alpha^2/2$ and $p = j\omega$, C becomes

$$C = \int_0^\infty \exp[-(u + x)] I_0(2\sqrt{xu}) e^{pu} du \quad (46)$$

Marcum found this integral to be (12:163-164)

$$C = [1/(p+1)] e^{-x} \exp[x/(p+1)] \quad (47)$$

Fehlner takes the inverse Fourier transform by contour integration and obtains

$$\begin{aligned} f(t) &= (1/2\pi j) \int_{-j\infty}^{j\infty} \frac{e^{-x} \exp[x/(p+1)] \exp[(p+1-1)t]}{p+1} dp \\ &= \frac{e^{-x} e^{-t}}{2\pi j} \int_{-j\infty}^{j\infty} \frac{\exp[-x/(p+1)] \exp[t(p+1)]}{p+1} dp \end{aligned} \quad (48)$$

Fehlner's evaluation of this integral results in

$$f(t) = e^{-x} \sum_{i=0}^{\infty} (x^i/i!)(t^i/i!) \quad (49)$$

Now, to determine the Q function, the integral

$$\int_{u_T}^{\infty} f(t) dt \quad (50)$$

must be evaluated, where u_T is the threshold corresponding to β from the original expression for the Q function. Upon evaluation of this integral, Fehlner's final result becomes a series expression given by (7:24-25)

$$Q(x, u_T) = e^{-x} \sum_{i=0}^{\infty} (x^i/i!) \sum_{j=0}^i (e^{-u_T} u_T^j/j!) \quad (51)$$

Recalling that $x = \alpha^2/2$, $u = v^2/2$, and thus $u_T = \beta^2/2$, equation 51 becomes

$$Q(\alpha, \beta) = \sum_{i=0}^{\infty} \sum_{j=0}^i e^{-\alpha^2/2} \frac{(\alpha^2/2)^i}{i!} e^{-\beta^2/2} \frac{(\beta^2/2)^j}{j!} \quad (52)$$

This series can be carried out to the desired precision.

4.2 Computational Problems

It can be seen from equation 19 that as b and P_{fa} are decreased, the second argument of the Q function, β , becomes large. Also, as the SCR is increased, α , the first argument of the Q function, becomes large. Large values of α and β become

computationally hard to handle in equation 52. The expression

$$X = \frac{e^{-a}(a)^k}{k!} \quad (53)$$

must be evaluated with $a = \alpha^2/2$ or $a = \beta^2/2$. Large values of α , β , and k cause numbers for X well outside the limitations of a computer.

This problem can be handled by first evaluating

$$\ln X = -a + k \ln a - \sum_{i=1}^k \ln i \quad (54)$$

This expression can be evaluated for large values of a and k (7:30-31). Then

$$X = \exp(\ln X) \quad (55)$$

Equation 52 becomes

$$Q(\alpha, \beta) = \sum_{i=0}^{\infty} \sum_{j=0}^i A_i B_j \quad (56)$$

where

$$\ln A_i = -\alpha^2/2 + i \ln(\alpha^2/2) - \sum_{k=1}^i \ln k \quad (57)$$

$$\ln B_j = -\beta^2/2 + j \ln(\beta^2/2) - \sum_{k=1}^j \ln k \quad (58)$$

$$A_i = \exp(\ln A_i) \quad (59)$$

$$B_j = \exp(\ln B_j) \quad (60)$$

Equation 56 can also be expressed as a recursive relationship where

$$Q(\alpha, \beta) = q_i \quad (61)$$

The initial value of q is computed as follows

$$\ln A_o = -\alpha^2/2 \quad (62)$$

$$\ln B_o = -\beta^2/2 \quad (63)$$

$$A_o = \exp(\ln A_o) \quad (64)$$

$$B_o = \exp(\ln B_o) \quad (65)$$

$$q_o = A_o B_o \quad (66)$$

The other values of q are computed from

$$\ln A_i = \ln A_{i-1} + \ln(\alpha^2/2) - \ln i \quad (67)$$

$$\ln B_i = \ln B_{i-1} + \ln(\beta^2/2) - \ln i \quad (68)$$

$$A_i = \exp(\ln A_i) \quad (69)$$

$$B_i = \exp(\ln B_i) \quad (70)$$

$$q_i = q_{i-1} + A_i B_i \quad (71)$$

The value of i in equation 61 must be large enough to cause Q to converge to the desired accuracy. To obtain a six digit accuracy, i must be large enough that

$$q_{i-1}/q_i > .999999 \quad (72)$$

4.3 Computer Program Design

The FORTRAN computer program found in Appendix A was developed to produce data that can be used to plot P_d versus SCR and P_d versus R/R_o for different values of b and P_{fa} . The input to the program includes: the value of b , the value of P_{fa} , and whether the grazing angle is large (beamwidth-limited case) or small (pulse-length-limited case).

The program evaluates equation 19, which is P_d expressed as the Q function

of $(\mathcal{R})^{1/2}$ and $[2\ln(1/P_{fa})]^{1/b}$. First α and β are computed according to equation 19. Then equations 62 through 66 are used to determine q_o . Then, a DO loop is carried out to determine q_i according to equations 67 through 71. The loop is exited when the inequality 72 is satisfied. Next, \mathcal{R} is converted to SCR according to equation 29. This conversion involves the Gamma function and the GAMMA function provided by the International Mathematical and Statistical Libraries (IMSL) is utilized in the program (10:GAMMA-1). R/R_o is then computed according to equation 38 or 39. The P_d , SCR, and R/R_o are output when P_d is between .0001 and .9999. Finally, \mathcal{R} is incremented and the computations are repeated until P_d becomes greater than .9999. The flow chart describing the program is shown in Figure 3.

Figures 4 through 12 are plots that show the required SCR needed to produce a desired P_d for various values of b and P_{fa} . Figures 13 through 21 are plots of P_d versus R/R_o for large grazing angles and Figures 22 through 30 are the same plots for small grazing angles.

As P_{fa} and b become small, the number of iterations required to cause the summation of equation 56 to converge becomes extremely large. The computation time required to evaluate the algorithm for small values of b and P_{fa} also becomes extremely large. This is why in Figures 11, 12, 20, 21, 29, and 30, the number of values of P_{fa} are limited. The skewness parameter, b , is reduced to .5 in Figures 12, 21, and 30. Values of b smaller than .506 are not documented.

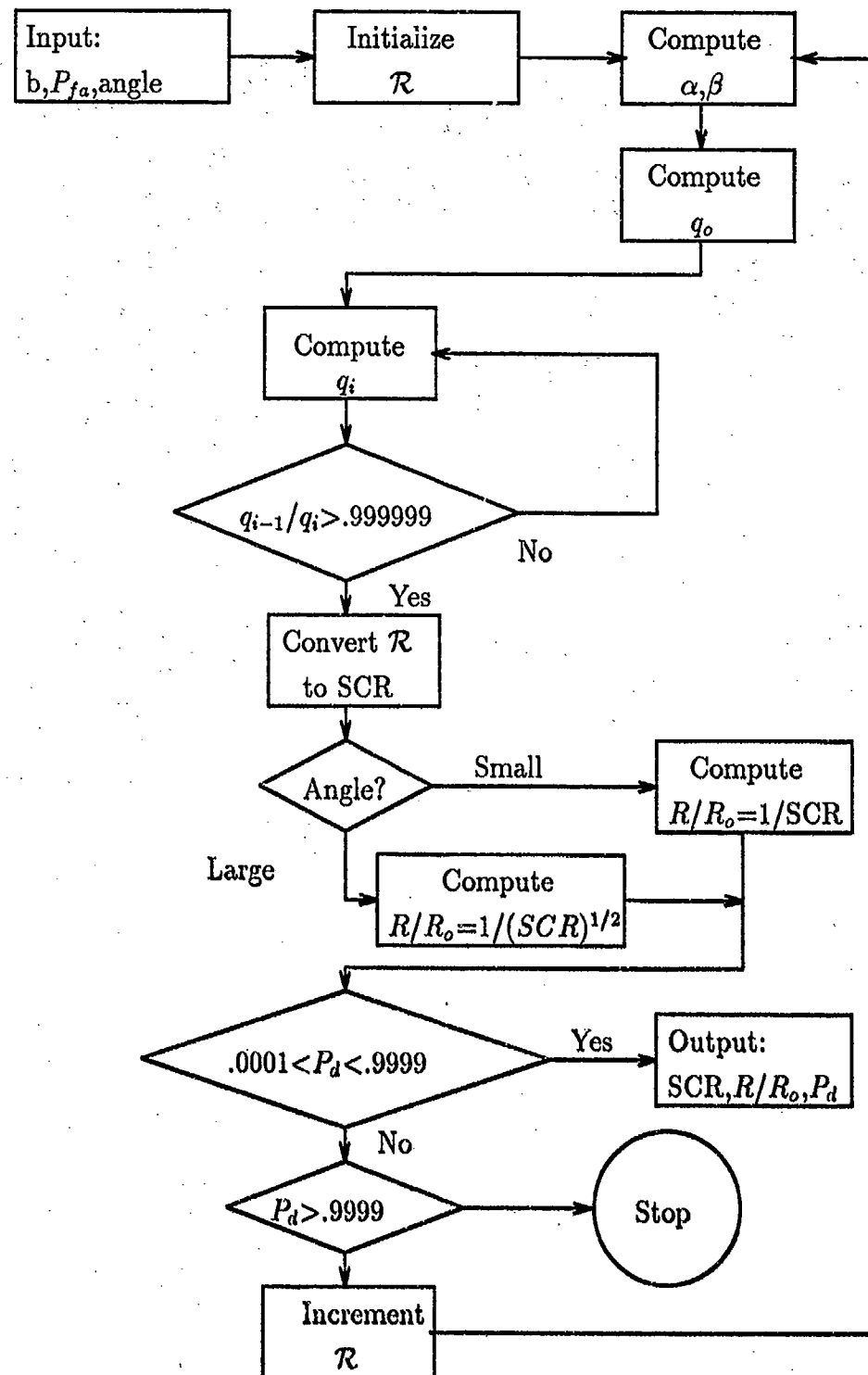


Figure 3. Program Flowchart

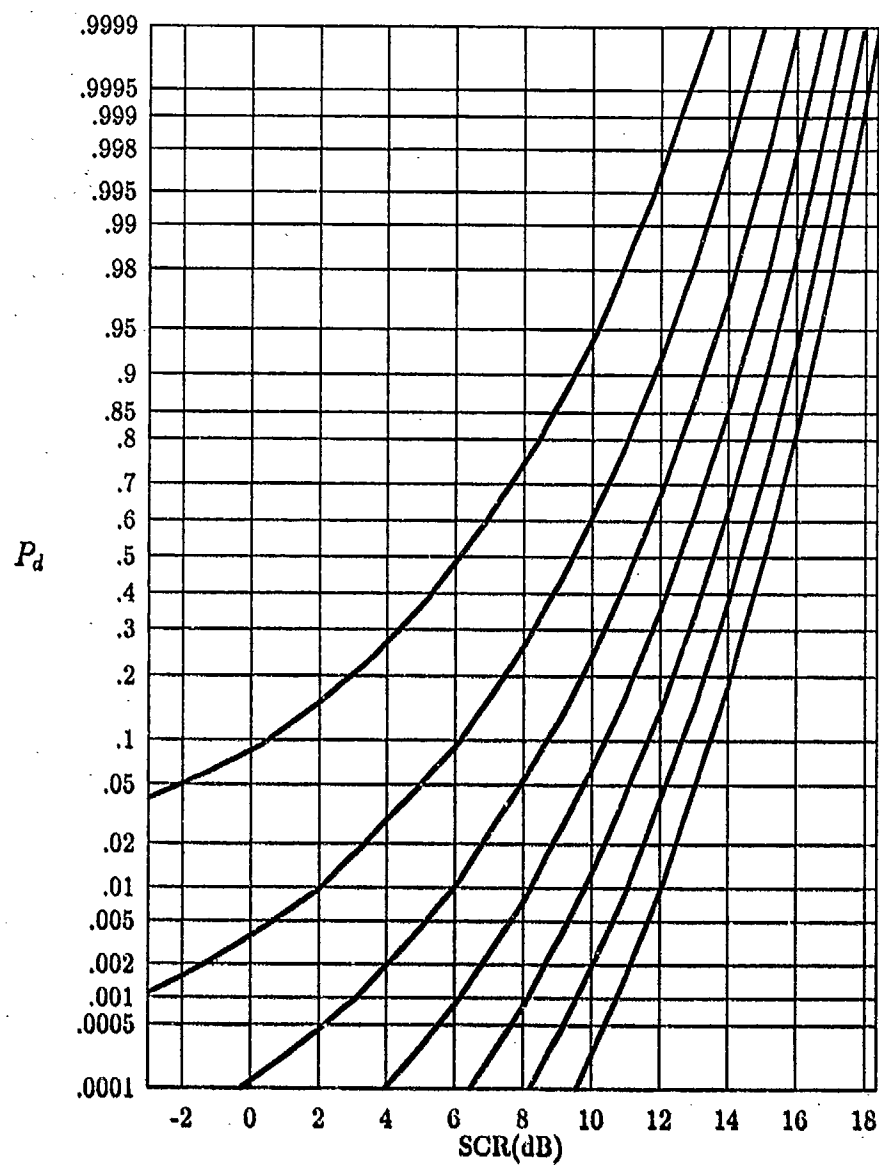


Figure 4. P_d versus SCR for $b = 2$,
 $P_{fa} = 10^{-2}, 10^{-4}, 10^{-6}, 10^{-8}, 10^{-10},$
 $10^{-12}, 10^{-14}$ (left to right)

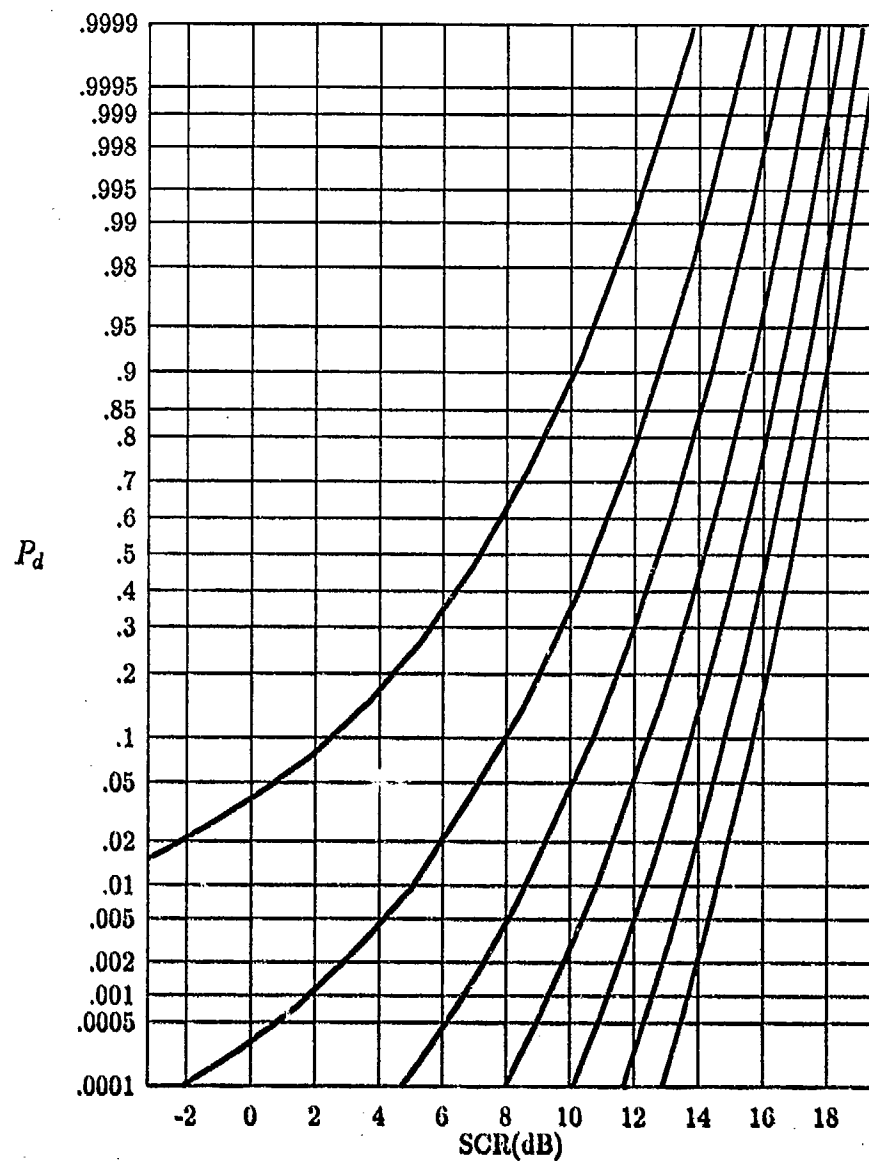


Figure 5. P_d versus SCR for $b = 1.8$,
 $P_{fa} = 10^{-2}, 10^{-4}, 10^{-6}, 10^{-8}, 10^{-10},$
 $10^{-12}, 10^{-14}$ (left to right)

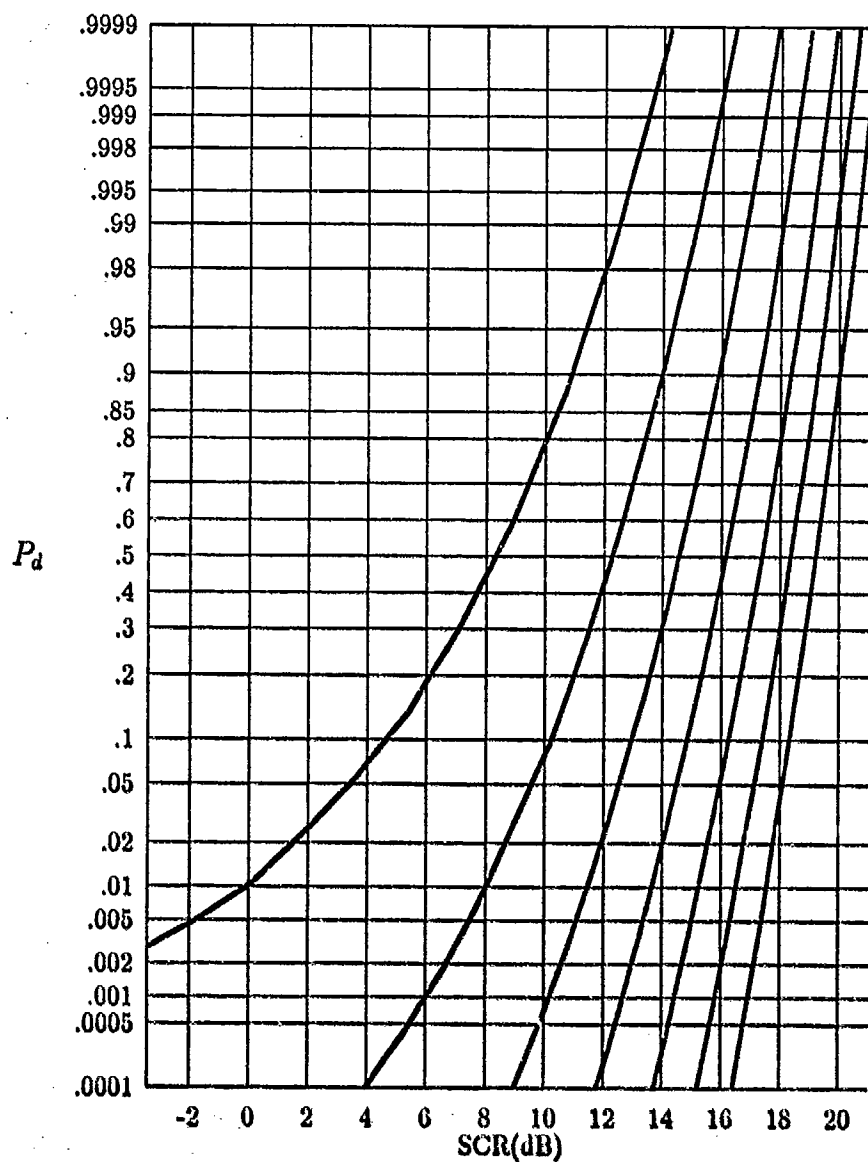


Figure 6. P_d versus SCR for $b = 1.6$,
 $P_{fa} = 10^{-2}, 10^{-4}, 10^{-6}, 10^{-8}, 10^{-10},$
 $10^{-12}, 10^{-14}$ (left to right)

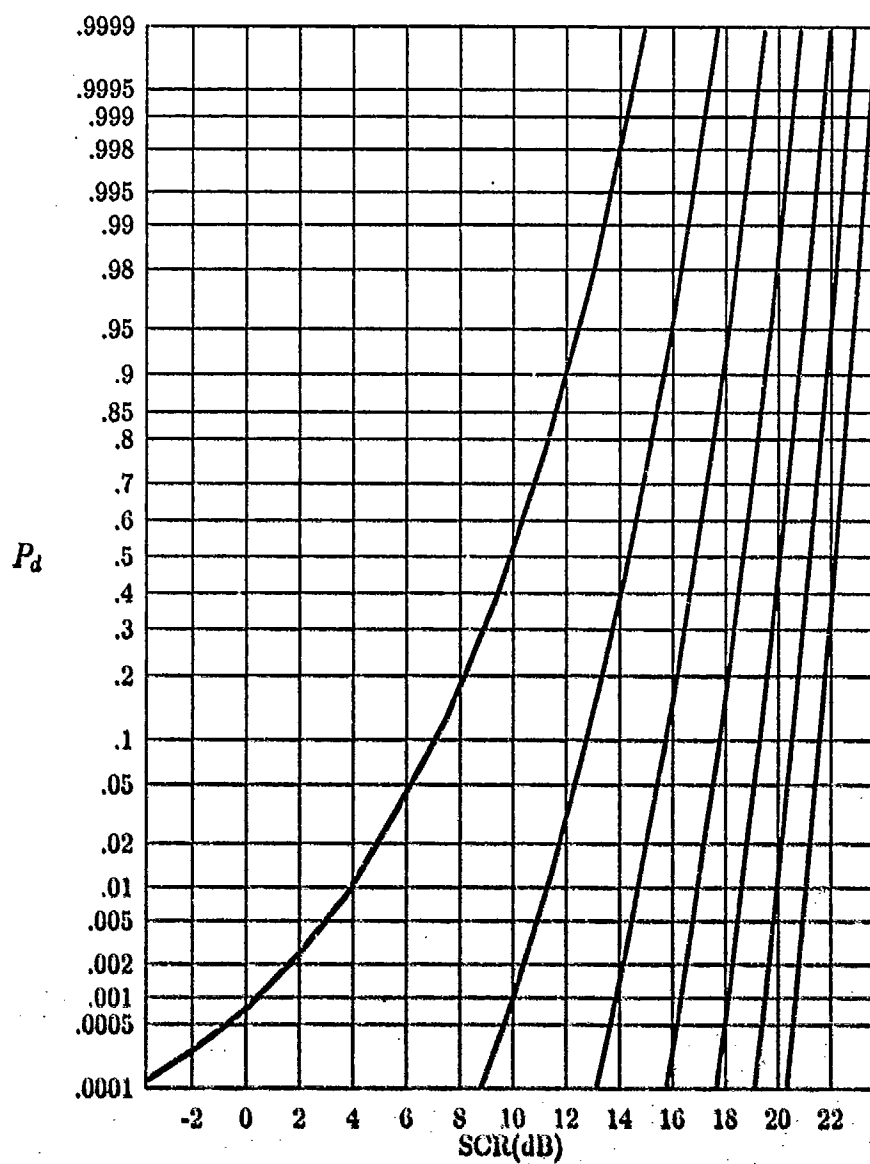


Figure 7. P_d versus SCR for $b = 1.4$,
 $P_{fa} = 10^{-2}, 10^{-4}, 10^{-6}, 10^{-8}, 10^{-10},$
 $10^{-12}, 10^{-14}$ (left to right)

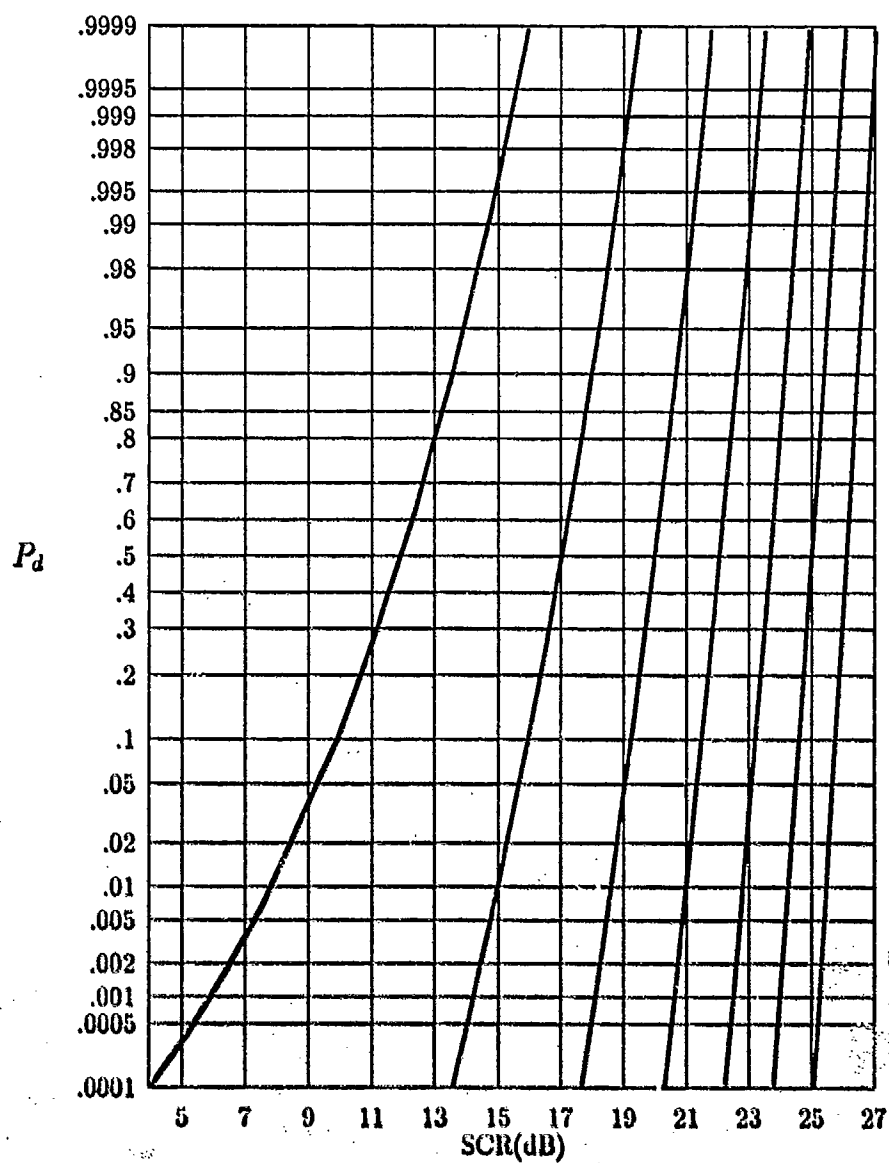


Figure 8. P_d versus SCR for $b = 1.2$,
 $P_{fa} = 10^{-2}, 10^{-4}, 10^{-6}, 10^{-8}, 10^{-10},$
 $10^{-12}, 10^{-14}$ (left to right)

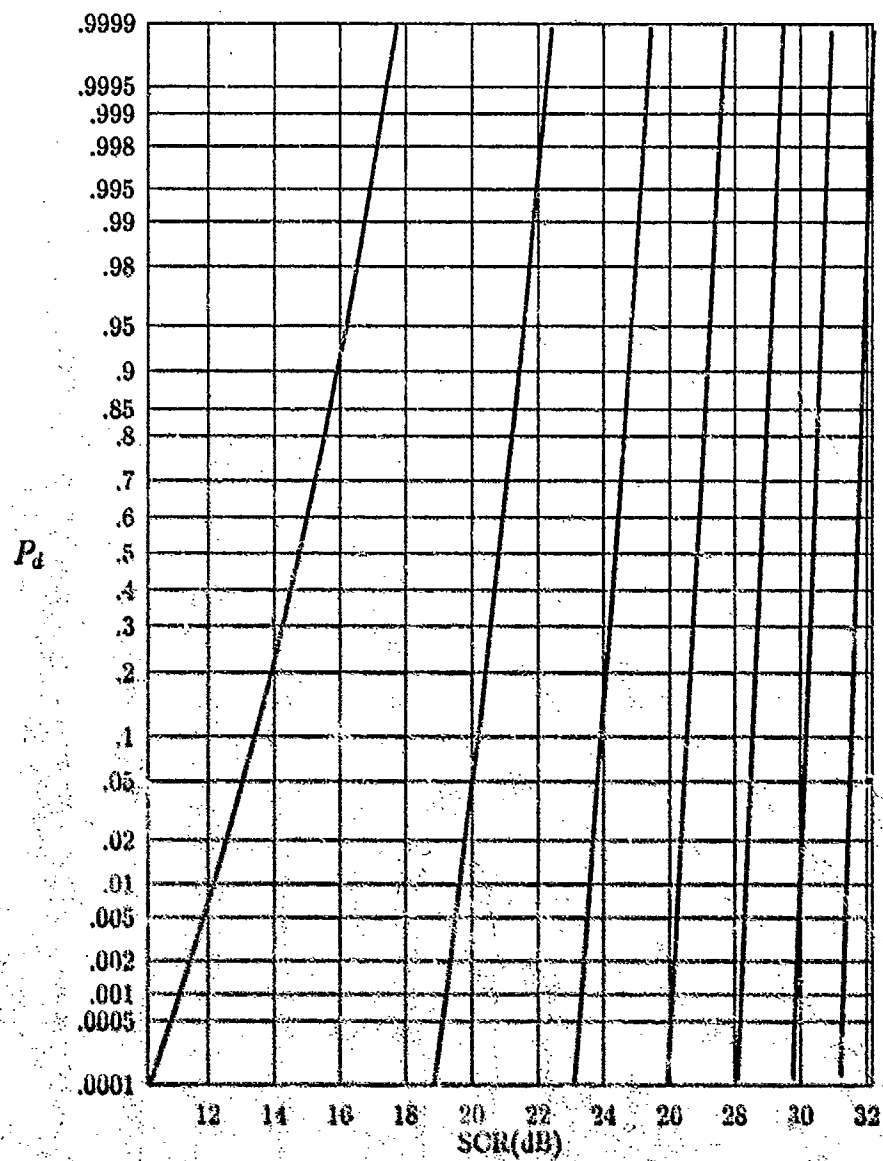


Figure 9. P_d versus SCR for $b = 1$,
 $P_{fa} = 10^{-2}, 10^{-4}, 10^{-6}, 10^{-8}, 10^{-10},$
 $10^{-12}, 10^{-14}$ (left to right)

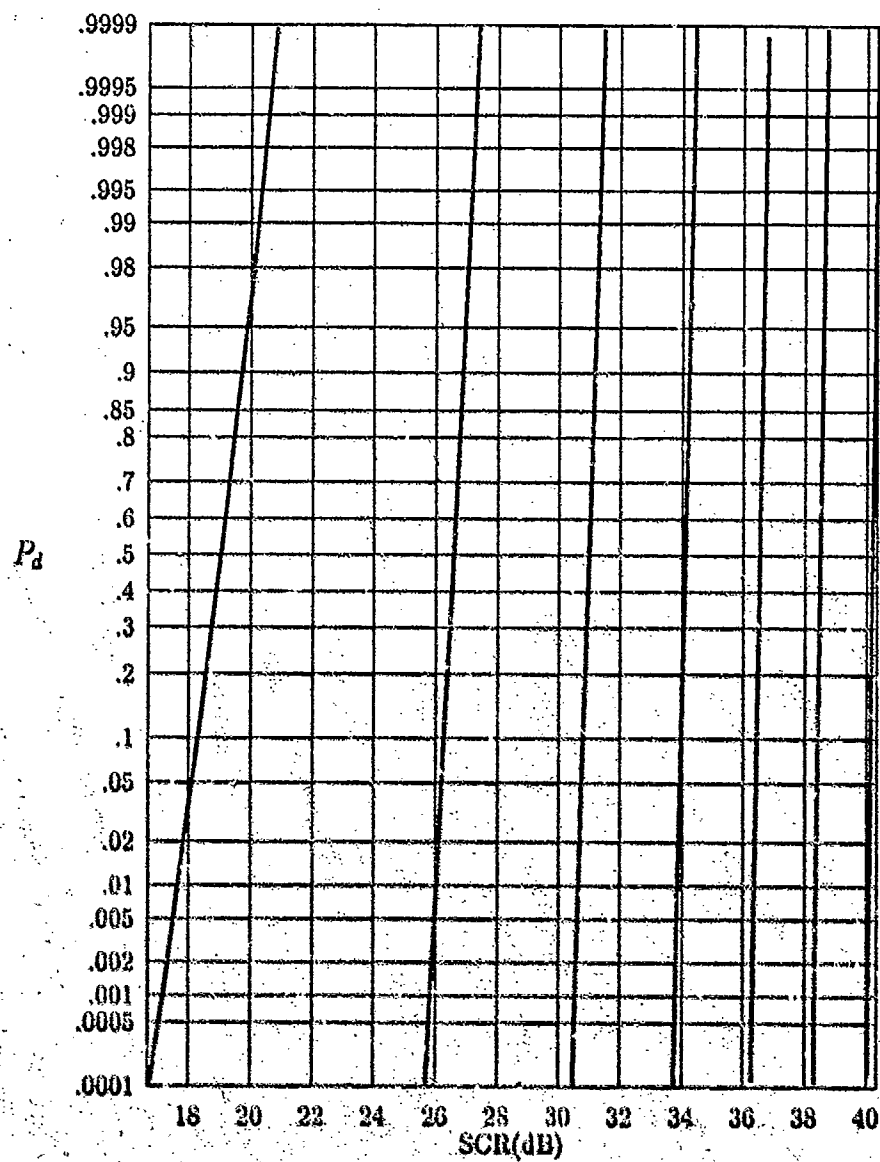


Figure 10. P_d versus SCR for $b = .8$,
 $P_{fa} = 10^{-2}, 10^{-4}, 10^{-6}, 10^{-8}, 10^{-10},$
 $10^{-12}, 10^{-14}$ (left to right)

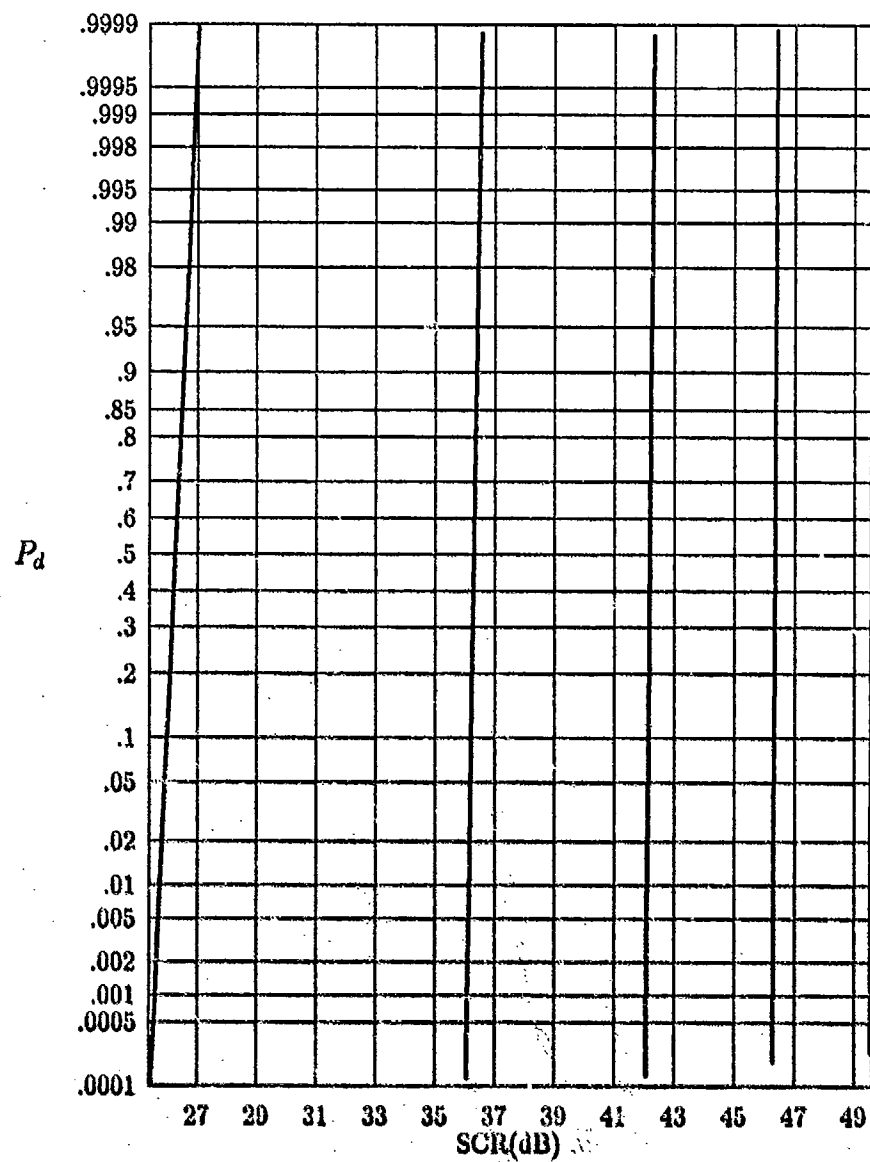


Figure 11. P_d versus SCR for $b = .6$,
 $P_{fa} = 10^{-2}, 10^{-4}, 10^{-6}, 10^{-8}, 10^{-10}$
 (left to right)

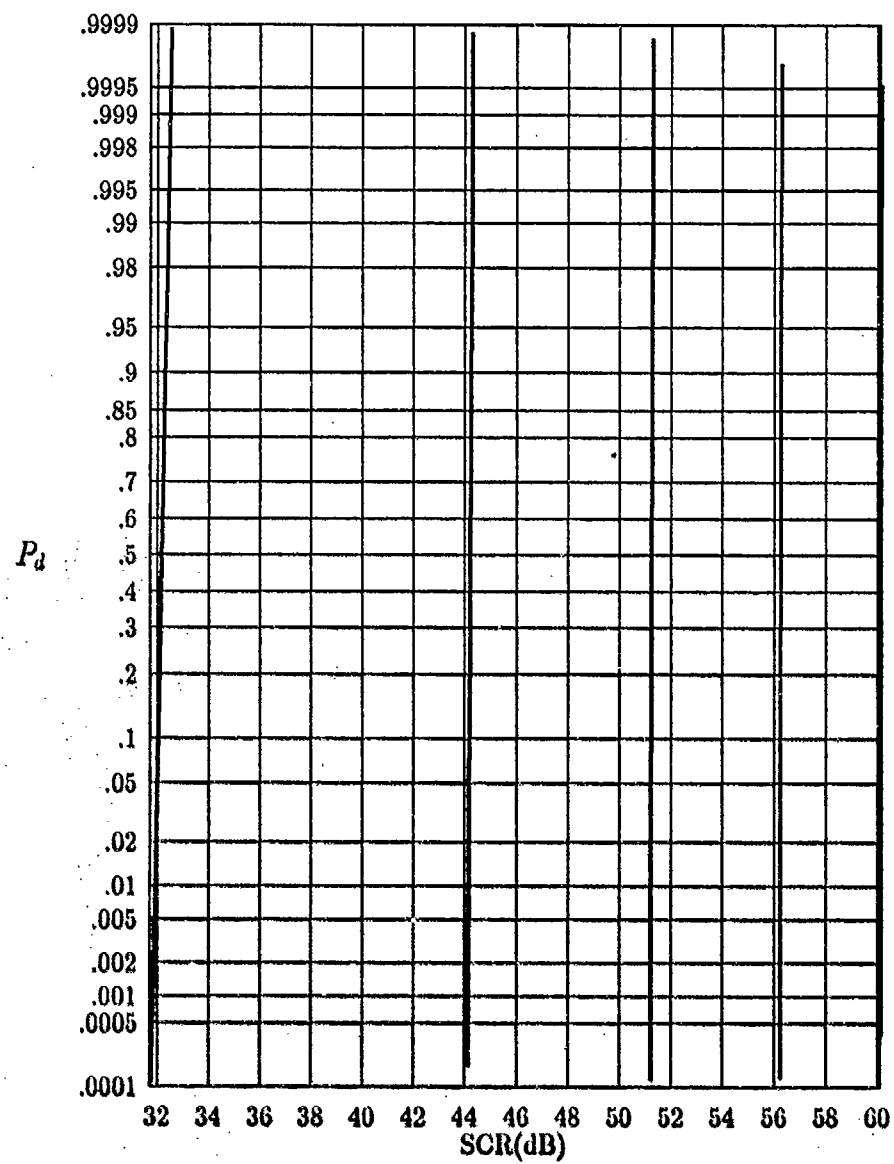


Figure 12. P_d versus SCR for $b = .5$,
 $P_{fa} = 10^{-2}, 10^{-4}, 10^{-6}, 10^{-8}, 10^{-10}$
 (left to right)

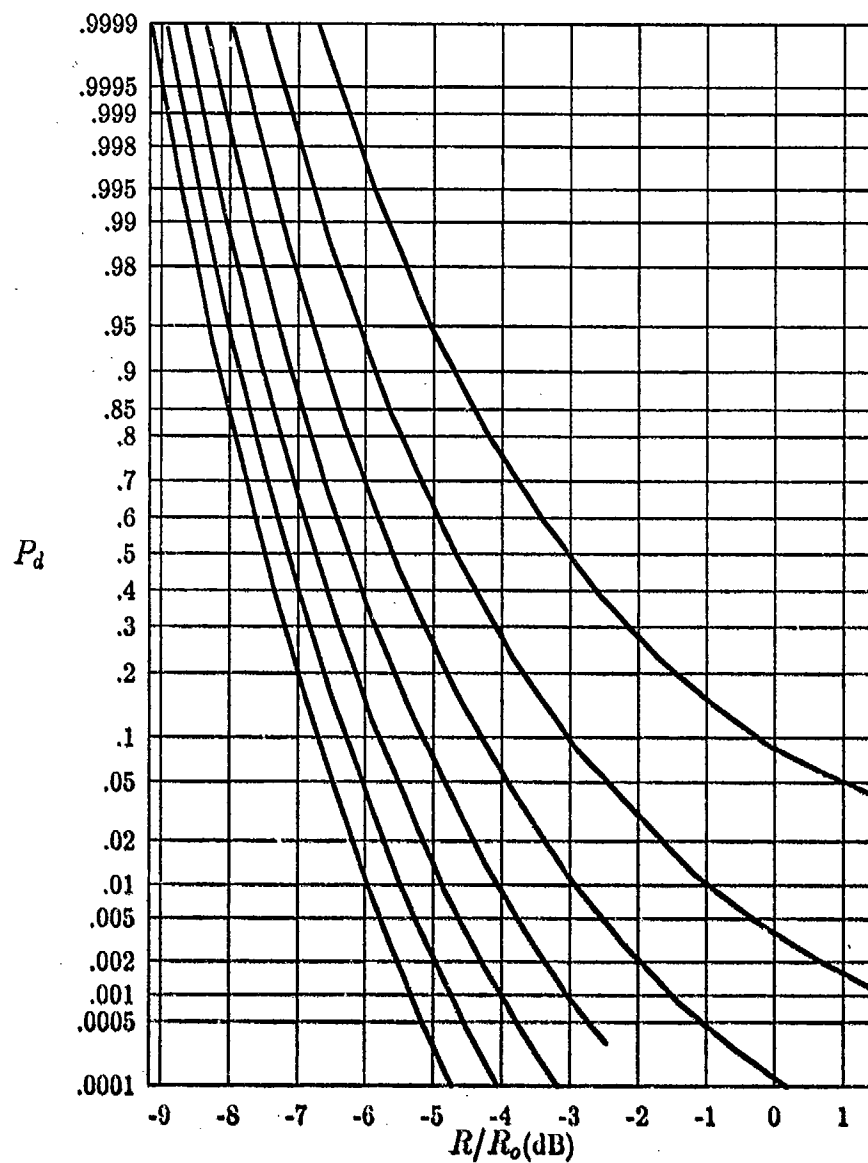


Figure 13. P_d versus R/R_o for $b = 2$ and large grazing angles,
 $P_{fa} = 10^{-2}, 10^{-4}, 10^{-6}, 10^{-8}, 10^{-10}, 10^{-12}, 10^{-14}$ (right to left)

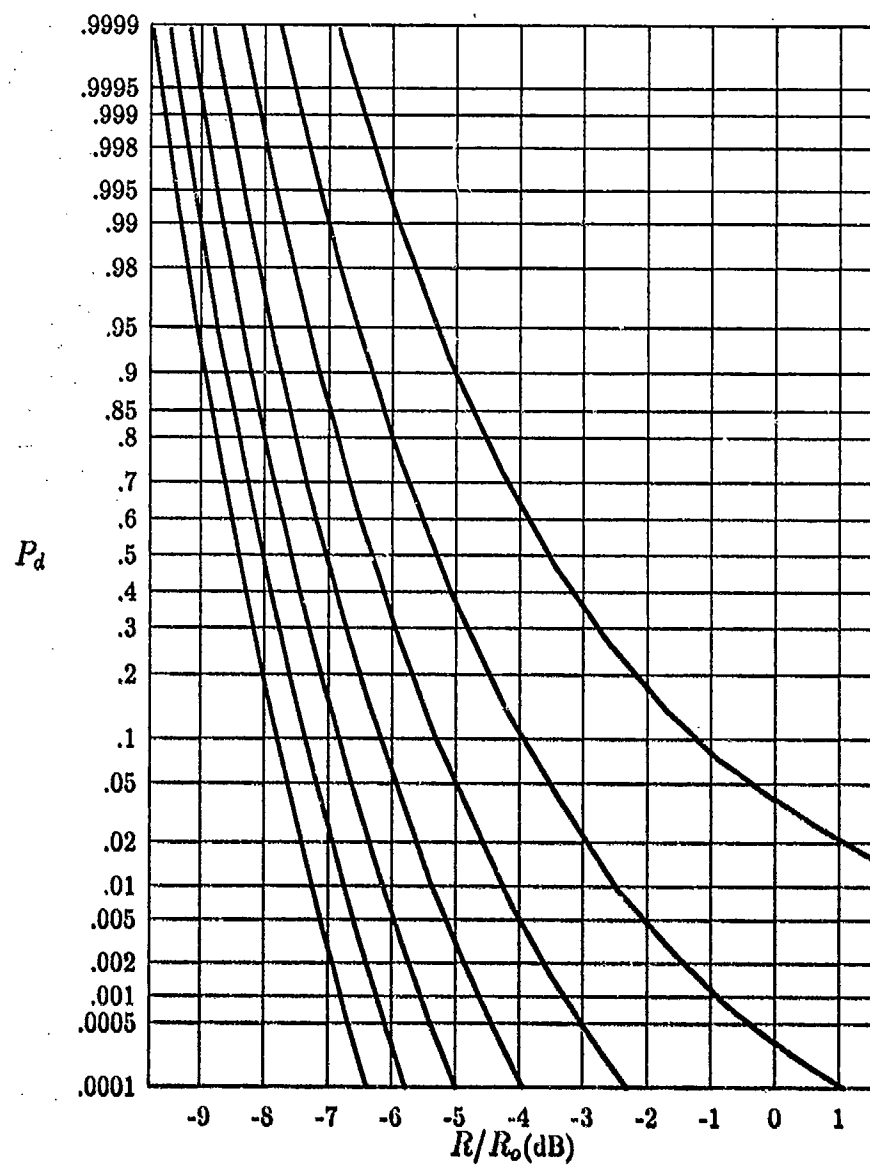


Figure 14. P_d versus R/R_o for $b = 1.8$ and large grazing angles,
 $P_{fa} = 10^{-2}, 10^{-4}, 10^{-6}, 10^{-8}, 10^{-10}, 10^{-12}, 10^{-14}$ (right to left)

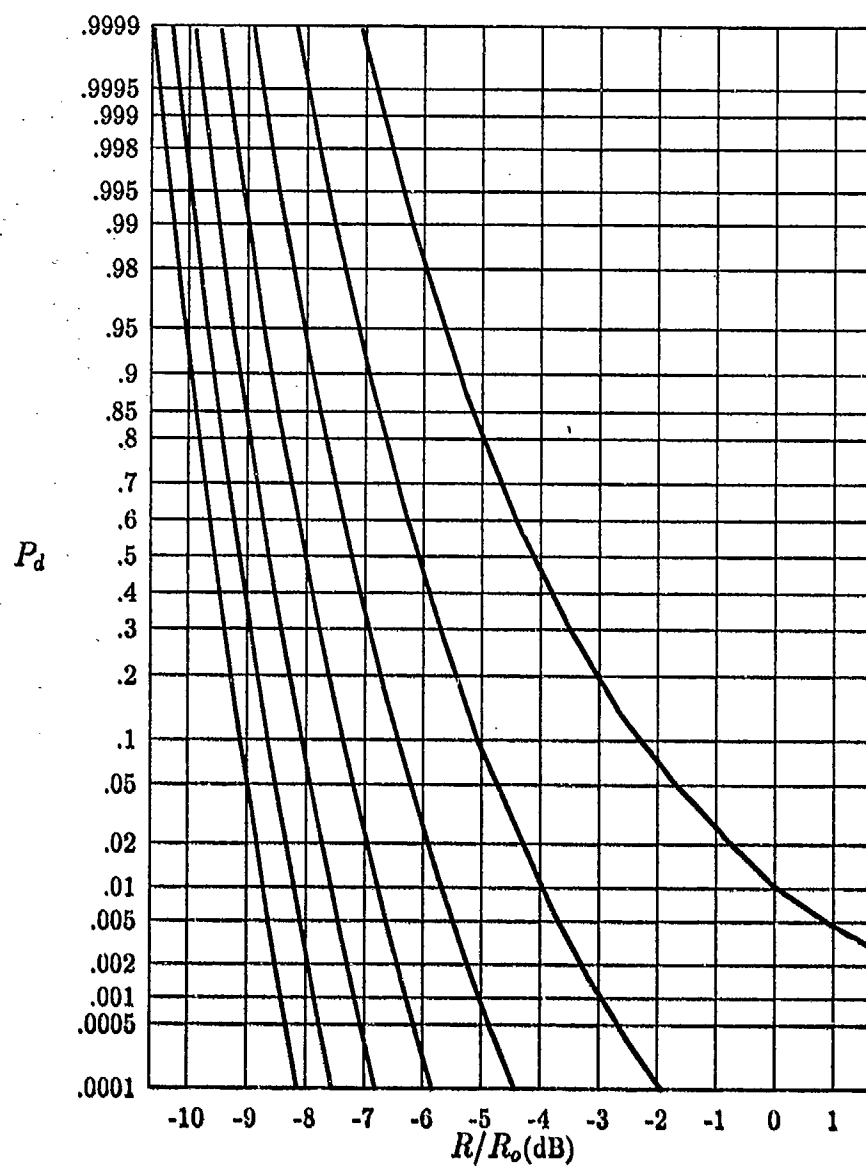


Figure 15. P_d versus R/R_o for $b = 1.6$ and large grazing angles,
 $P_{fa} = 10^{-2}, 10^{-4}, 10^{-6}, 10^{-8}, 10^{-10}, 10^{-12}, 10^{-14}$ (right to left)

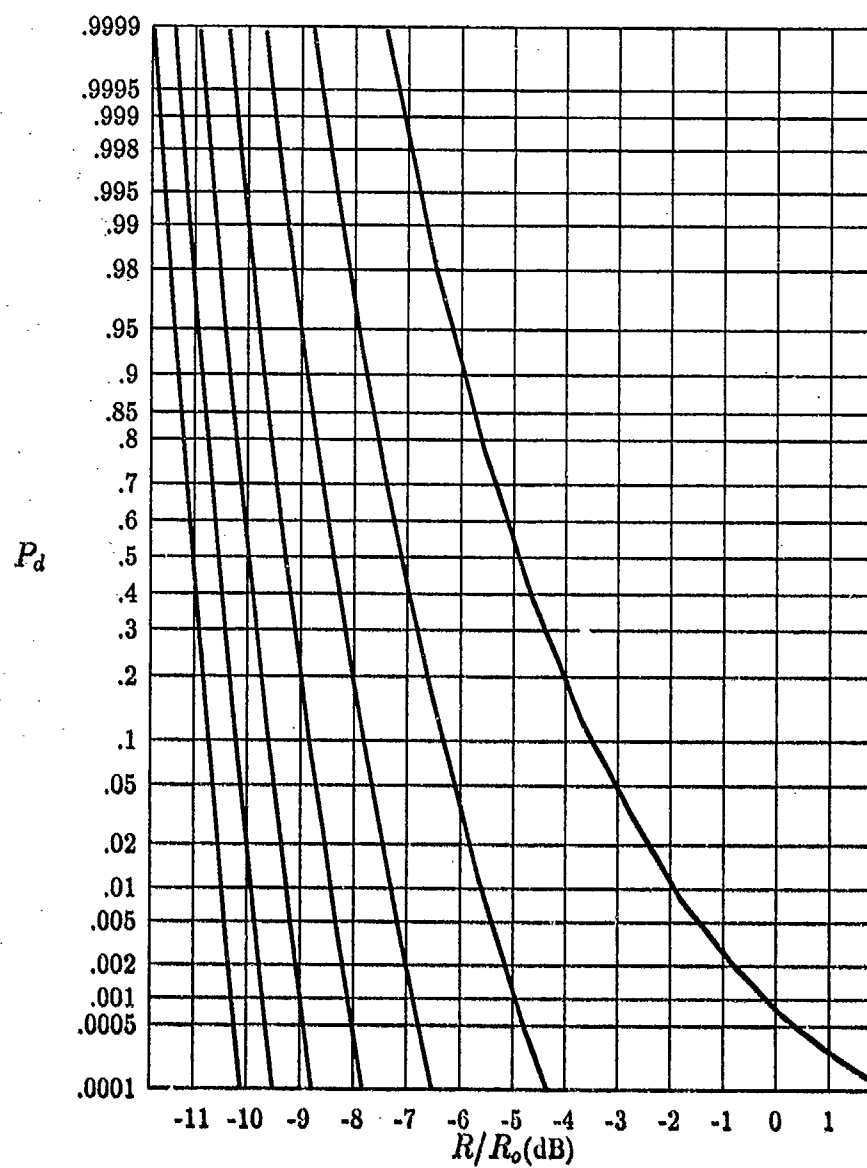


Figure 16. P_d versus R/R_o for $b = 1.4$ and large grazing angles,
 $P_{fc} = 10^{-2}, 10^{-4}, 10^{-6}, 10^{-8}, 10^{-10}, 10^{-12}, 10^{-14}$ (right to left)

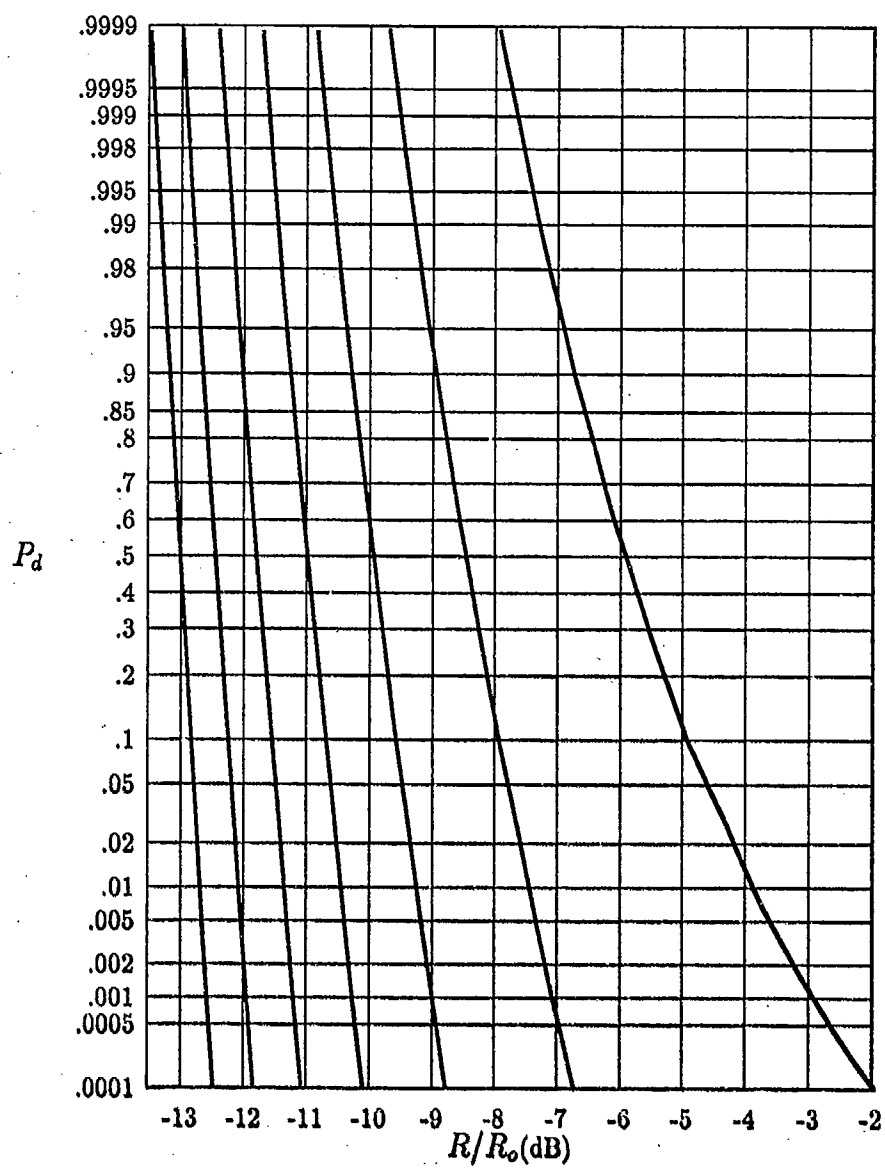


Figure 17. P_d versus R/R_o for $b = 1.2$ and large grazing angles,
 $P_{fa} = 10^{-2}, 10^{-4}, 10^{-6}, 10^{-8}, 10^{-10}, 10^{-12}, 10^{-14}$ (right to left)

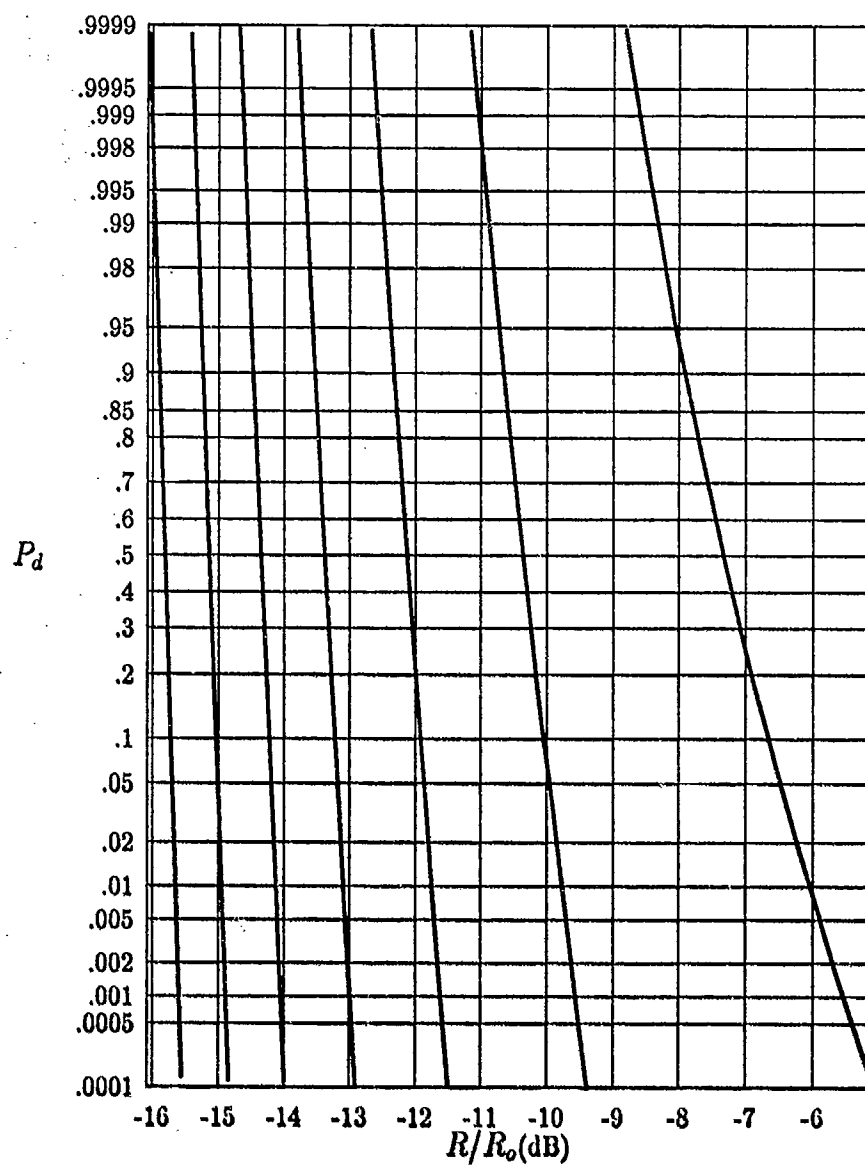


Figure 18. P_d versus R/R_o for $b = 1$ and large grazing angles,
 $P_{fa} = 10^{-2}, 10^{-4}, 10^{-6}, 10^{-8}, 10^{-10}, 10^{-12}, 10^{-14}$ (right to left)

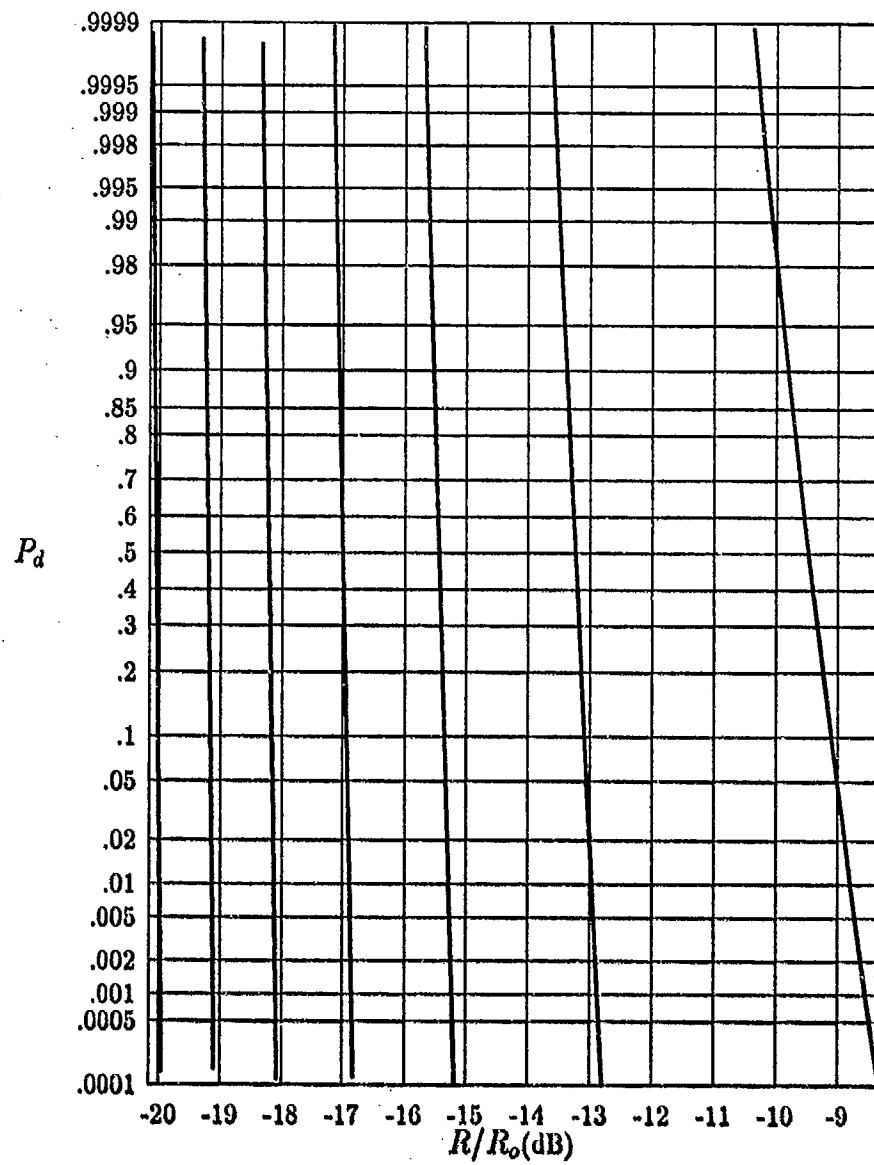


Figure 19. P_d versus R/R_o for $b = .8$ and large grazing angles,
 $P_{fa} = 10^{-2}, 10^{-4}, 10^{-6}, 10^{-8}, 10^{-10}, 10^{-12}, 10^{-14}$ (right to left)

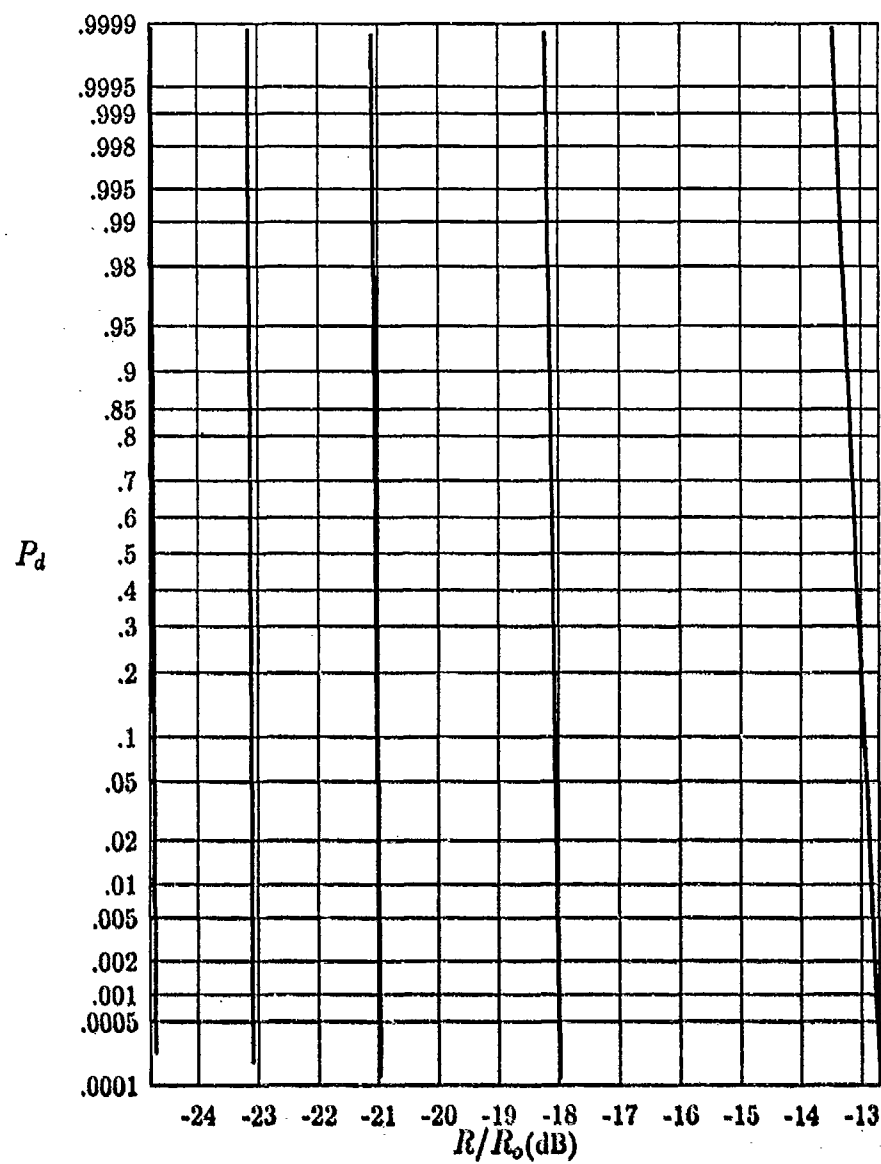


Figure 20. P_d versus R/R_o for $b = .6$ and large grazing angles,
 $P_{fa} = 10^{-2}, 10^{-4}, 10^{-6}, 10^{-8}, 10^{-10}$ (right to left)

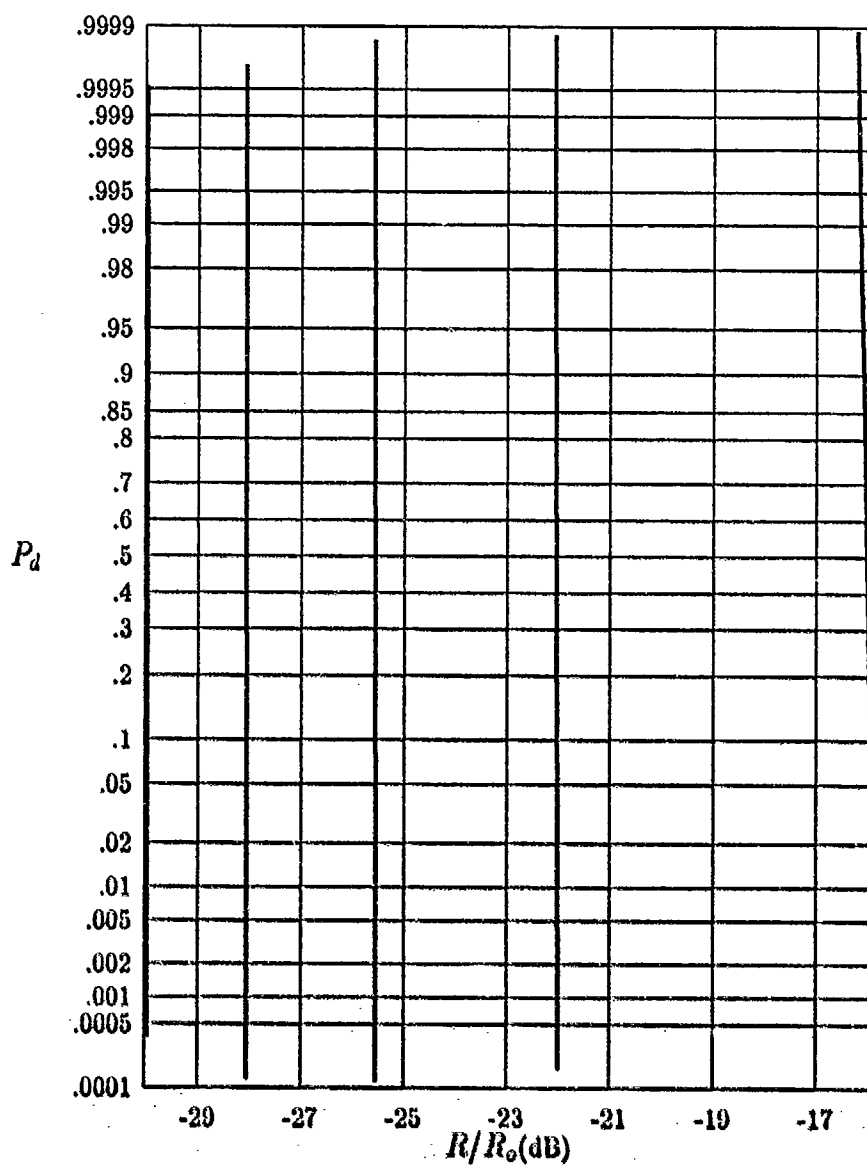


Figure 21. P_d versus R/R_o for $b = .5$ and large grazing angles,
 $P_{fa} = 10^{-2}, 10^{-4}, 10^{-6}, 10^{-8}, 10^{-10}$ (right to left)

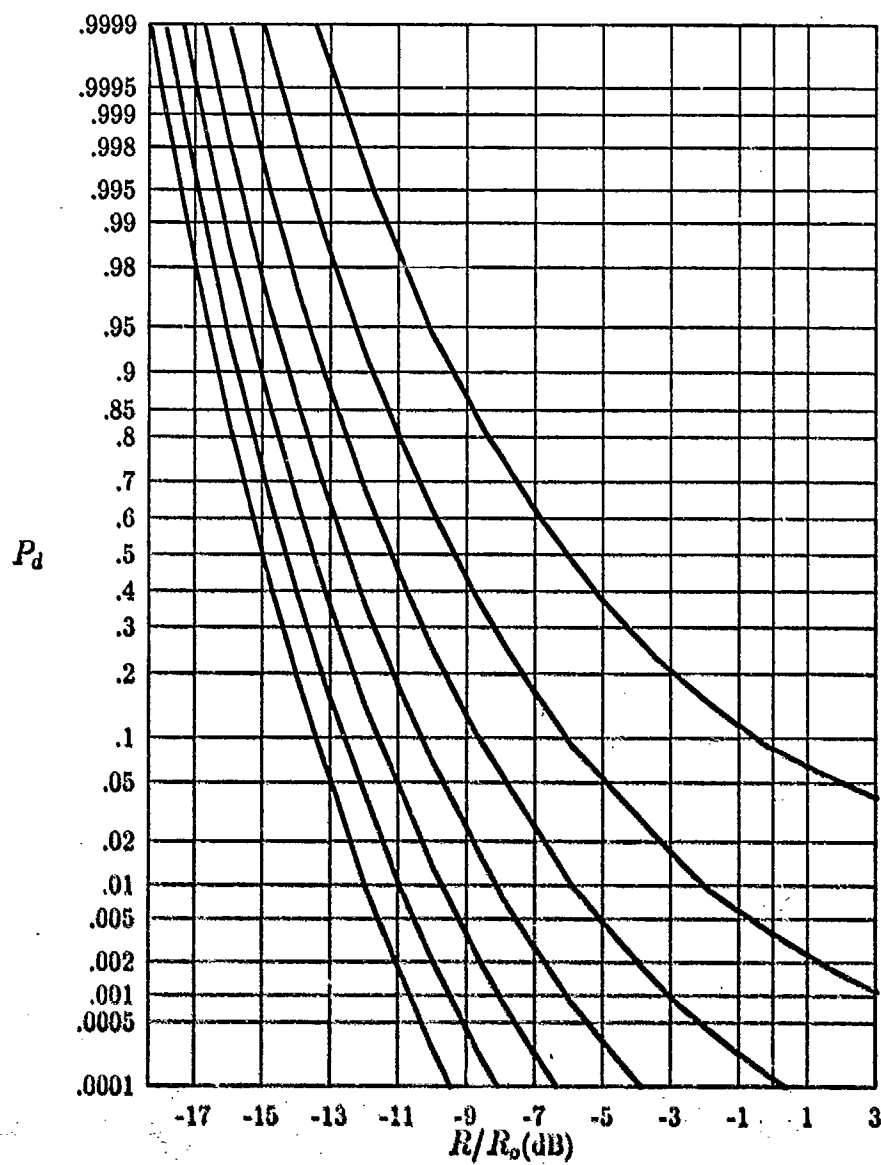


Figure 22. P_d versus R/R_o for $b = 2$ and small grazing angles,
 $P_{f0} = 10^{-2}, 10^{-4}, 10^{-6}, 10^{-8}, 10^{-10}, 10^{-12}, 10^{-14}$ (right to left)

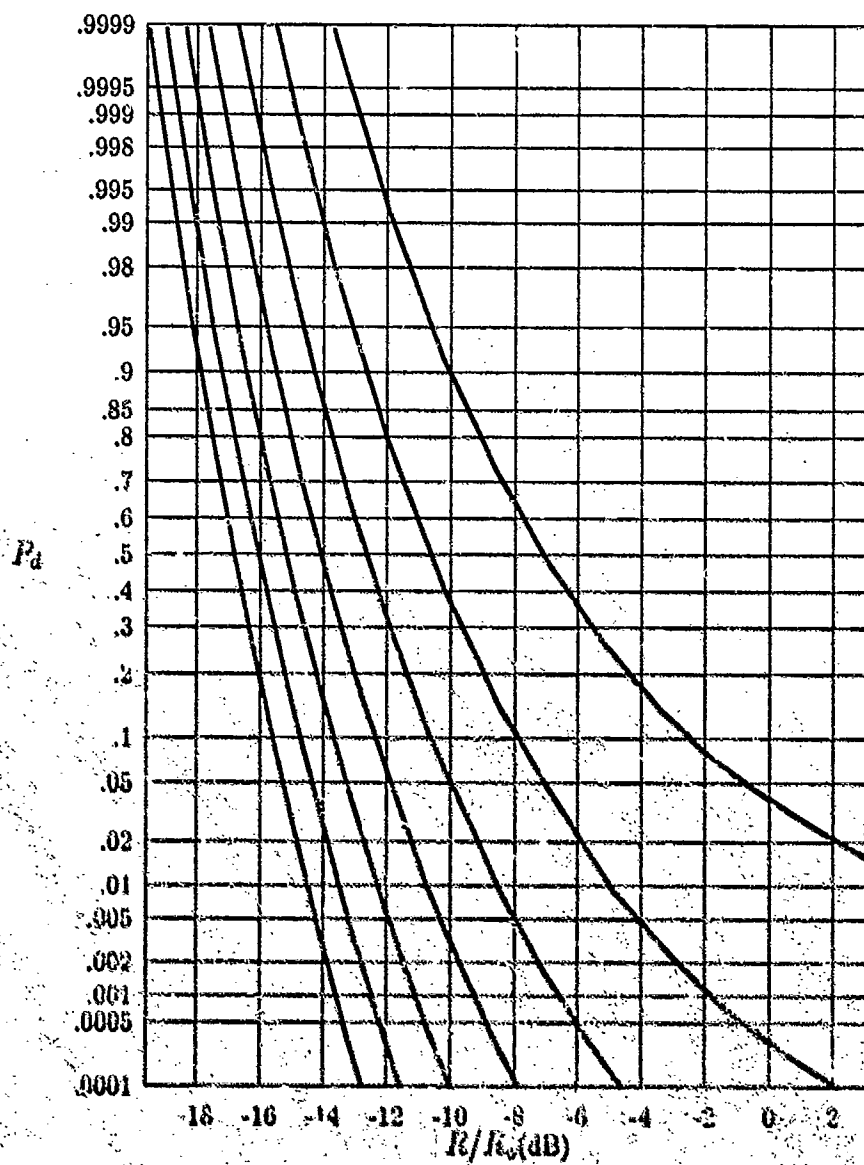


Figure 23. P_d versus R/R_0 for $b = 1.8$ and small grazing angles;
 $P_{f0} = 10^{-2}, 10^{-4}, 10^{-6}, 10^{-8}, 10^{-10}, 10^{-12}, 10^{-14}$ (right to left).

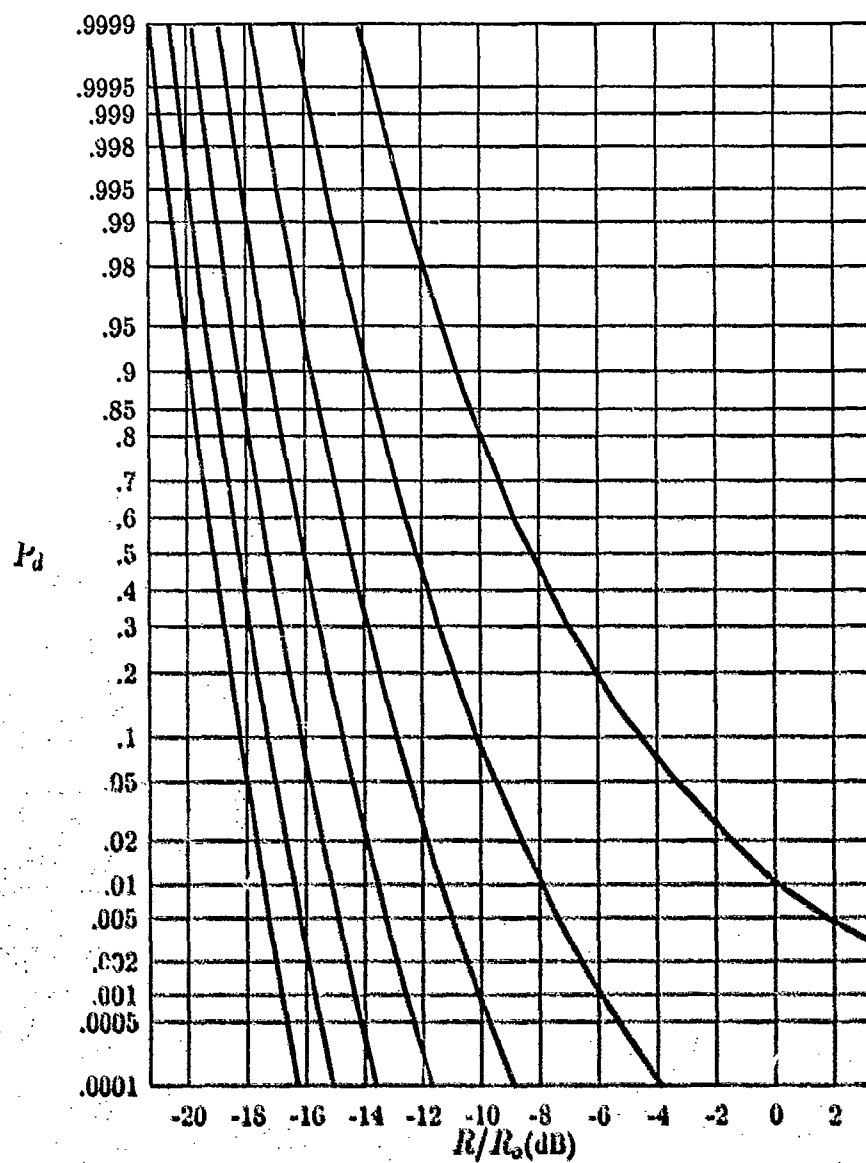


Figure 24. P_d versus R/R_0 for $b = 1.6$ and small grazing angles,
 $P_{fa} = 10^{-2}, 10^{-4}, 10^{-6}, 10^{-8}, 10^{-10}, 10^{-12}, 10^{-14}$ (right to left)

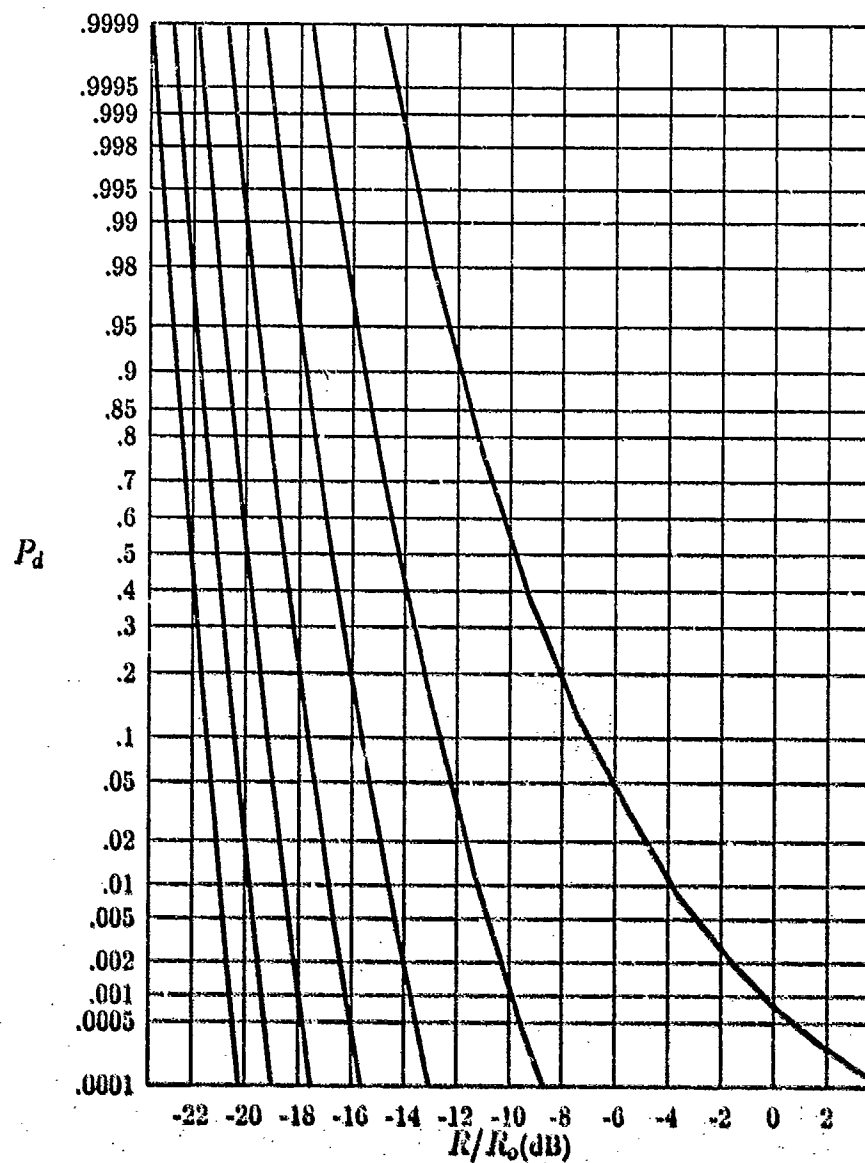


Figure 25. P_d versus R/R_0 for $b = 1.4$ and small grazing angles,
 $P_{Ja} = 10^{-2}, 10^{-4}, 10^{-6}, 10^{-8}, 10^{-10}, 10^{-12}, 10^{-14}$ (right to left)

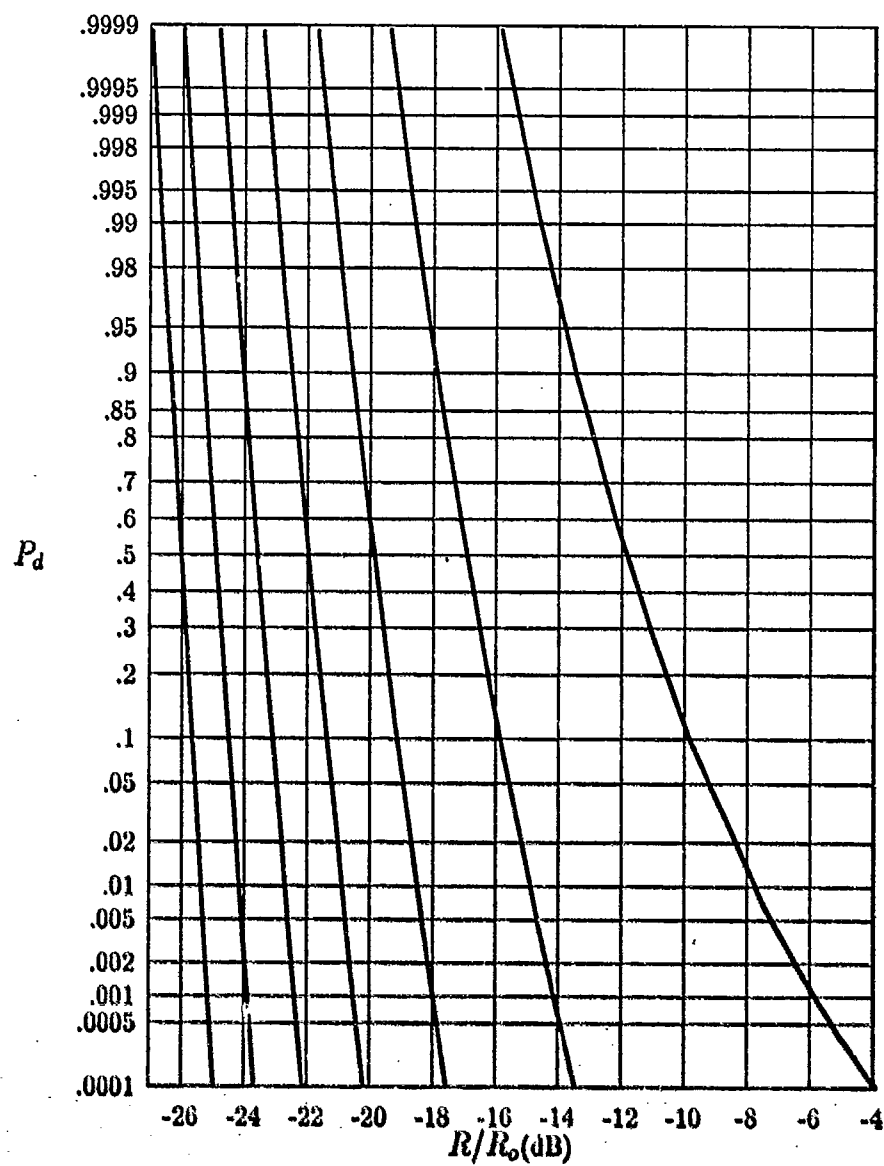


Figure 26. P_d versus R/R_o for $b = 1.2$ and small grazing angles,
 $P_{fa} = 10^{-2}, 10^{-4}, 10^{-6}, 10^{-8}, 10^{-10}, 10^{-12}, 10^{-14}$ (right to left)

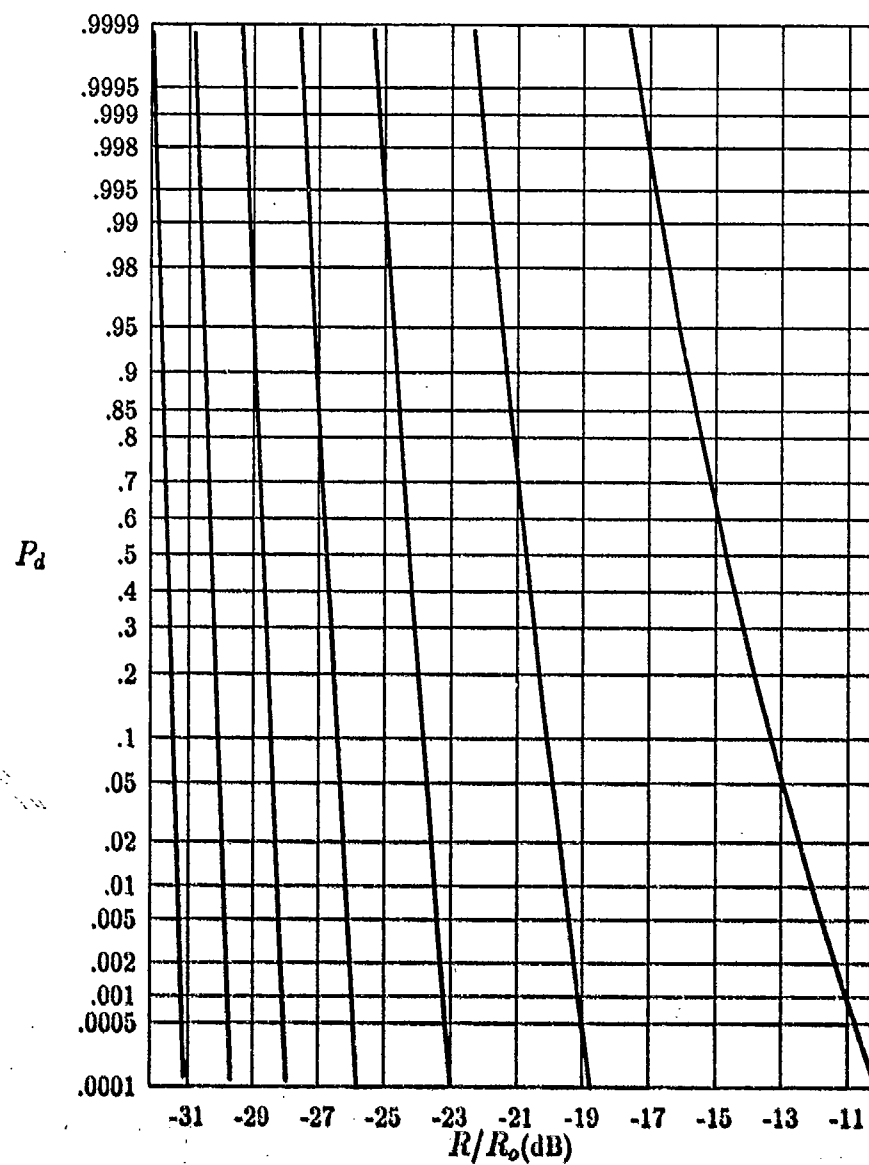


Figure 27. P_d versus R/R_o for $b = 1$ and small grazing angles,
 $P_{fa} = 10^{-2}, 10^{-4}, 10^{-6}, 10^{-8}, 10^{-10}, 10^{-12}, 10^{-14}$ (right to left)

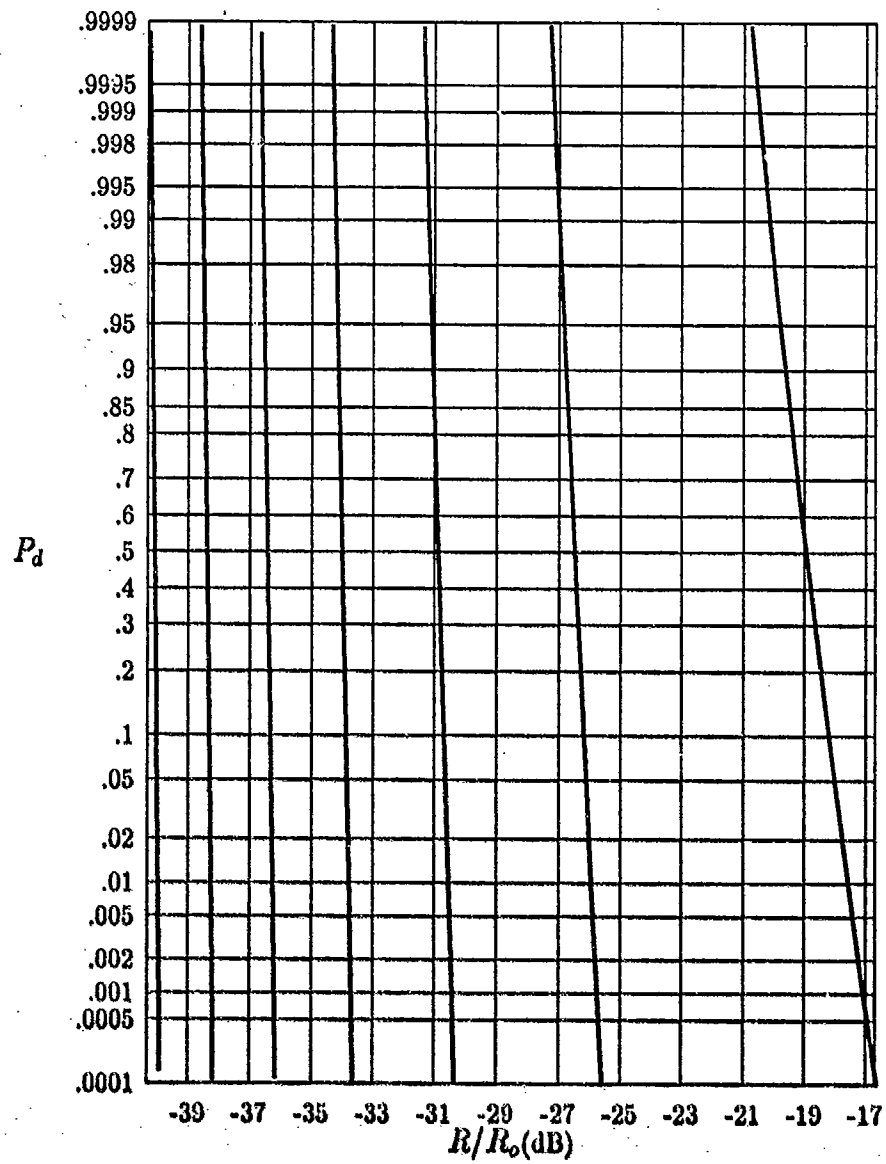


Figure 28. P_d versus R/R_o for $b = .8$ and small grazing angles,
 $P_{f0} = 10^{-2}, 10^{-4}, 10^{-6}, 10^{-8}, 10^{-10}, 10^{-12}, 10^{-14}$ (right to left)

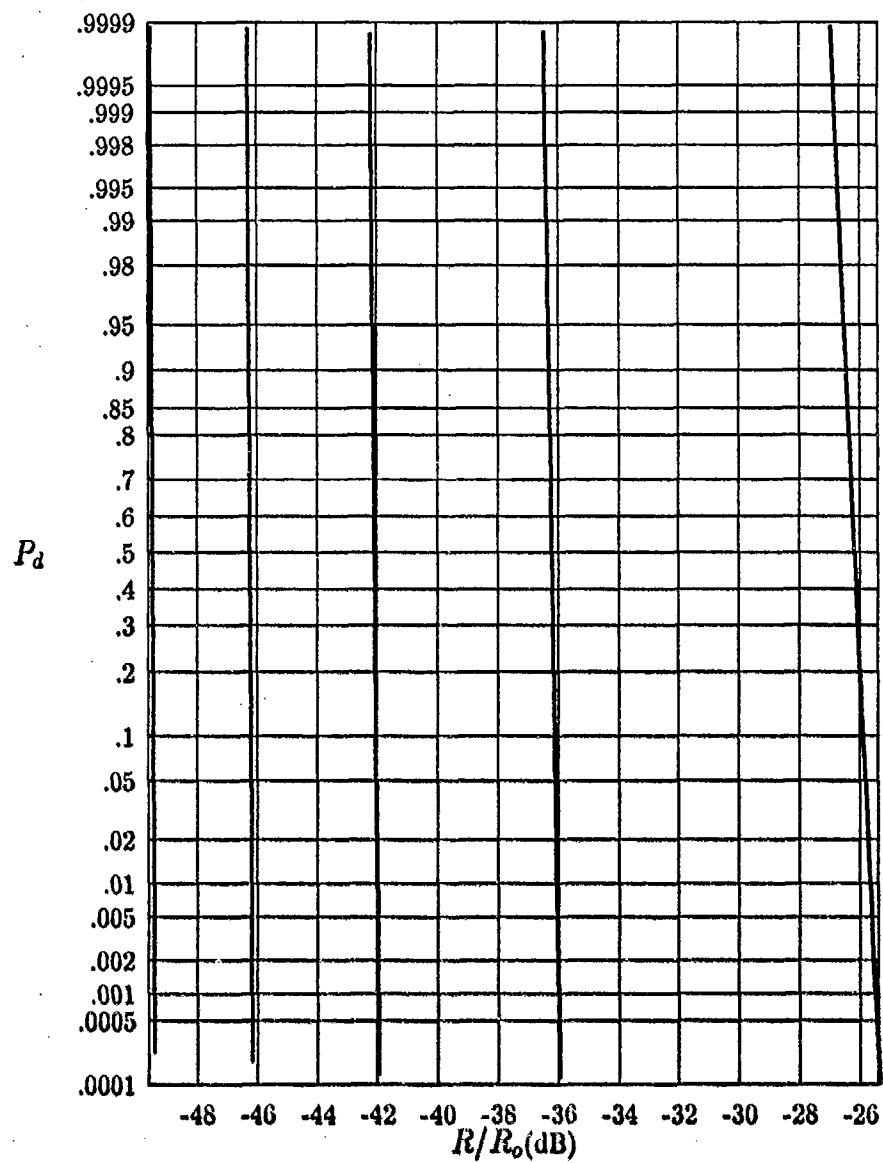


Figure 29. P_d versus R/R_o for $b = .6$ and small grazing angles, $P_{fa} = 10^{-2}, 10^{-4}, 10^{-6}, 10^{-8}, 10^{-10}$ (right to left)

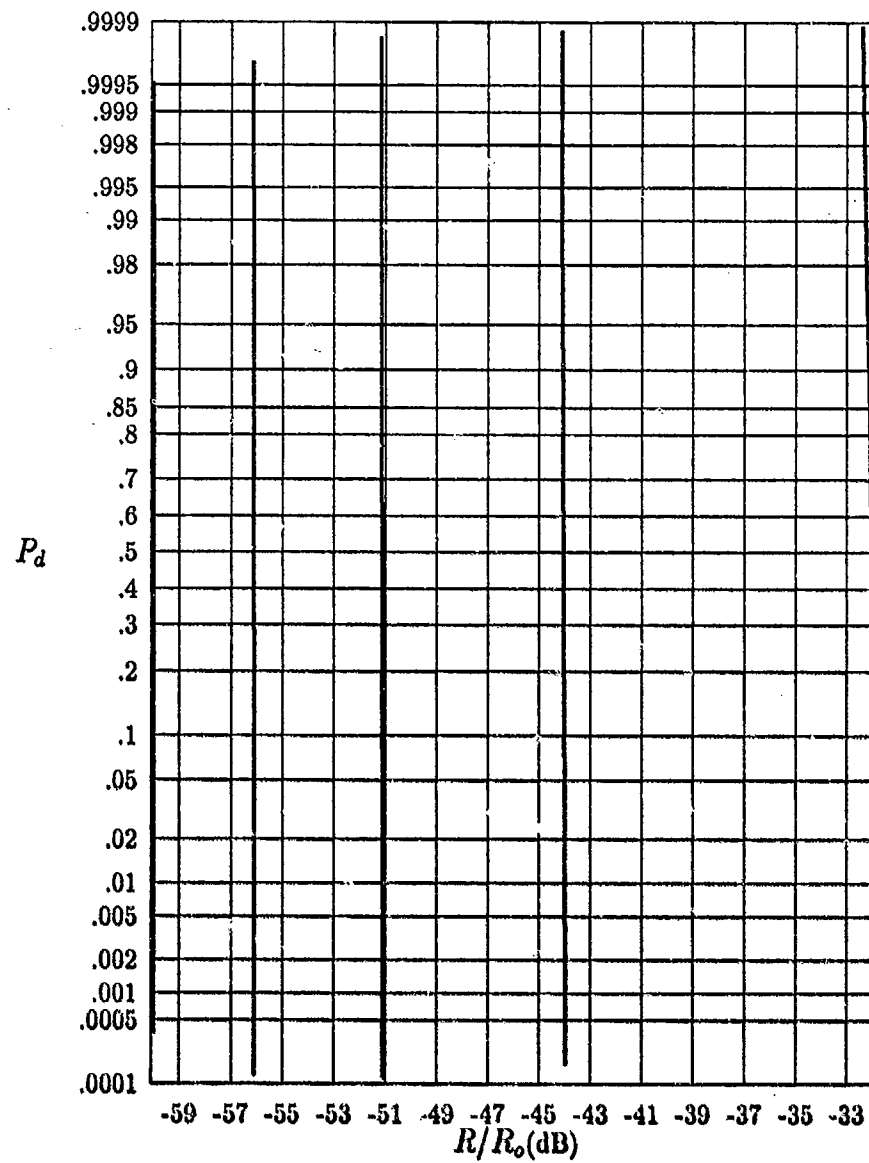


Figure 30. P_d versus R/R_o for $b = .5$ small grazing angles,
 $P_{fa} = 10^{-2}, 10^{-4}, 10^{-6}, 10^{-8}, 10^{-10}$ (right to left)

4.4 Results

4.4.1 Validation. In order to determine if the curves presented are valid, the curves developed for $b = 2$ can be compared to those presented by other authors who analyzed the detection problem of a steady target in Gaussian noise. When $b = 2$, the pdf of the envelope of the interference is Rayleigh as seen from equation 7, and Rayleigh envelope interference corresponds to Gaussian noise at the input to an envelope detector. Therefore, the detection problem for a steady target in Weibull clutter with $b = 2$ is identical to the problem of detecting a steady target in Gaussian noise. DiFranco and Rubin's curves of P_d versus the peak signal-to-noise ratio for the Gaussian detection problem are identical to the curves shown in Figure 4 except for a 3 dB shift in the peak signal-to-noise ratio axis (5:308). This discrepancy is explained by noting that the curves in Figure 4 are plotted with the mean signal-to-clutter ratio, SCR, on the x-axis while DiFranco and Rubin use the peak signal-to-noise ratio, \mathcal{R} . From equation 28, it can be seen that when $b = 2$, $SCR = \mathcal{R}/2$, thus the 3 dB discrepancy.

To further validate the curves, they can be compared to the results obtained by Schleher. Schleher developed plots of P_d versus SCR for a steady target in Weibull clutter for $P_{fa} = 10^{-6}$ and $b = 2, 1.2, .8$, and $.6$ (18:737-739). These plots correspond to the curves shown in Figures 4, 8, 10, and 11 with $P_{fa} = 10^{-6}$ and the curves in these figures match the ones developed by Schleher.

4.4.2 Comparison of Results for Various Values of b . From the results obtained, it is seen that as b is decreased, or the skewness of the clutter distribution is decreased, the amount of SCR required to produce a desired P_d is increased and thus the detection range is decreased. Table 2 shows the additional SCR required to produce a $P_d = .9$ with $P_{fa} = 10^{-6}$ when b is not equal to 2 compared to the Rayleigh envelope case when $b = 2$. The decrease in range for large and small grazing angles is also shown. Table 2 shows that as the skewness of the clutter distribution is changed

Table 2. Additional SCR and Decrease in Detection Range

b	Additional SCR(dB)	Decrease in R/R_o for Small Grazing Angles(dB)	Decrease in R/R_o for Large Grazing Angles(dB)
1.8	1.2	1.2	.6
1.6	2.6	2.6	1.3
1.4	4.6	4.6	2.3
1.4	4.6	4.6	2.3
1.2	7.4	7.4	3.7
1	11.6	11.6	5.8
.8	17.8	17.8	8.9
.6	28.6	28.6	14.3
.5	38	38	19

(b decreases), the performance of the envelope detector receiver is degraded.

As an example of the performance degradation, one can compare the detection characteristics found for two different types of terrain. Suppose $b = .626$ for terrain characterized by wooded hills and $b = 1.452$ for the ocean (see Table 1). Using the algorithm and computer program described previously, it was found that approximately 24.1 dB more SCR is needed to detect a steady target over wooded hills than that needed to detect a steady target over the ocean. For small grazing angles, the detection range is also 24.1 dB less for detection over wooded hills than the ocean and for large grazing angles, the detection range is decreased by 12.03 dB.

V. Conclusions and Recommendations

5.1 Conclusions

The purpose of this thesis was to develop a means of predicting the radar detection range of steady targets in Weibull clutter. This was accomplished by modifying a detection scheme used to detect steady targets in Gaussian noise and then determining the relationship between P_d , P_{fa} , SCR, and b and finally applying this relationship to a modified form of the radar range equation. The expressions describing the relationship between P_d , P_{fa} , SCR, b , and range were found to be in the form of Marcum's Q function (see equations 31, 40, and 42). Computer implementation of the recursive algorithm presented in Chapter 4 used for the evaluation of the Q function was capable of producing data used to plot P_d versus SCR and P_d versus range for various values of P_{fa} and b . Six digit precision was used in developing the plots but the algorithm is capable of providing greater accuracy.

The plots of P_d versus SCR developed in Chapter 4 describe the detection characteristics of a steady target in Weibull clutter and show that the performance of the detector is severely degraded as the skewness of the clutter distribution is decreased. That is, as b is decreased, the SCR required to produce desired values of P_d and P_{fa} becomes large (see Table 2).

Finally, the plots of P_d versus R/R_0 provide a means of predicting the radar detection range for particular types of clutter (values of b) and desired values of P_d and P_{fa} . Several improvements can be made to this study and some are suggested in the next section.

5.2 Recommendations for Future Research

5.2.1 Weibull Target. The next step in the Weibull clutter detection problem is to allow the target to fluctuate. The Weibull pdf can be used to model the target

just as it was used to model the radar clutter. Recall that the Weibull target model is equivalent to the often used Rayleigh model when $b = 2$. The Weibull target model is better suited than the steady target model as an approach to problems like detecting helicopters flying nap of the earth profiles. The following development is provided as a suggestion on how to approach the analysis of Weibull target detection in Weibull clutter.

With the problem of detecting a Weibull target in Weibull clutter, the pdf of the detected signal under the hypothesis of clutter alone present is still given by equation 7. When a target is immersed in clutter, the pdf of the detected signal describes the distribution of the sum of two random processes. The pdf of the sum of two random variables is the convolution of the individual pdfs (4:186-189). The pdf corresponding to the clutter is

$$p_c(w) = (b_o/\alpha_o)w^{b_o-1} \exp(-w^{b_o}/\alpha_o) \quad w > 0 \quad (73)$$

and the pdf corresponding to the target is

$$p_t(w) = (b_1/\alpha_1)w^{b_1-1} \exp(-w^{b_1}/\alpha_1) \quad w > 0 \quad (74)$$

so the pdf of the signal under the hypothesis that a target is present becomes

$$p(w/H_1) = p_c(w) * p_t(w) \quad (75)$$

Therefore the pdfs of the detected signal under the alternate hypotheses are

$$p(w/H_o) = (b_o/\alpha_o)w^{b_o-1} \exp(-w^{b_o}/\alpha_o) \quad w > 0 \quad (76)$$

$$p(w/H_1) = \frac{b_o b_1}{\alpha_o \alpha_1} \int_0^w w^{b_o-1} (w-x)^{b_1-1} \exp(-w^{b_o}/\alpha_o) \exp[-(w-x)^{b_1}/\alpha_1] dx \quad (77)$$

The parameters b_0 and α_0 pertain to the clutter while b_1 and α_1 pertain to the target.

The integral in equation 77 cannot be expressed in closed form, making it difficult to determine the P_d . The integral can be approximated numerically using techniques such as the trapezoidal rule or Simpson's rule (11:368-390). The pdf of equation 77 can then be evaluated for a range of values of w and the distribution corresponding to the pdf of 77 becomes a discrete distribution.

Proceeding using a binary decision approach, the likelihood ratio, $\Lambda(w)$, can be written as

$$\Lambda(w) = \frac{p(w/H_1)}{p(w/H_0)} \quad (78)$$

and the likelihood ratio test becomes

$$\Lambda(w) = \frac{p(w/H_1)}{p(w/H_0)} \begin{matrix} >_{H_1} \\ <_{H_0} \end{matrix} \lambda \quad (79)$$

where λ is determined by the particular decision criteria that is employed. Using the Neyman-Pearson decision criteria which requires that λ be determined according to a preselected value of P_{fa} , the detection threshold, w_T , can be found by equation 11 and λ becomes (13:28-38)

$$\lambda = \Lambda(w_T) \quad (80)$$

When dealing with discrete distributions, the P_d can be determined by summing up $p(w_i/H_1)$ for all i such that $\Lambda(w_i) > \Lambda(w_T)$ (17). That is

$$P_d = \sum_i p(w_i/H_1) \text{ such that } \Lambda(w_i) > \Lambda(w_T) \quad (81)$$

where $p(w_i/H_1)$ is determined from the numerical evaluation of equation 77, $p(w_i/H_0)$ is determined from equation 76, $\Lambda(w_i)$ is determined from equation 78, and w_i can

be any value between 0 and infinity. Equation 81 can also be written as

$$P_d = 1 - \sum_i p(w_i/H_1) \text{ such that } \Lambda(w_i) < \Lambda(w_T) \quad (82)$$

The details of performing the numerical integration, developing the discrete distribution, finding the relationship between P_d , P_{fa} , and SCR, and applying the results to the radar range equation are left to future researchers.

5.2.2 Other Recommendations. Future research should examine the target detection problem with more than one observation of the returned pulse. That is, instead of using single-hit detection, utilize pulse integration in the detection scheme and examine the problem with multiple pulse observations.

Also, the problem could be extended by determining the detection characteristics when other types of radar are used. A comparison of the detection characteristics could be made for pulse, moving target indicator (MTI), pulse doppler, and continuous wave (CW) radars.

5.3 Summary

By using the expressions for P_d developed in Chapter 3 and the algorithm for evaluating these expressions presented in Chapter 4, the detection characteristics of a steady target in Weibull clutter can be determined. P_d can be found to a desired precision for varying values of SCR, R/R_o , P_{fa} , and b and plots can be developed which show the relationship between P_d , P_{fa} , SCR, and the radar detection range. Finally, the radar detection range of steady targets in Weibull clutter can be predicted by examining the plots of P_d versus R/R_o .

Appendix A. Computer Program Listing

```

C *****
C *
C *      THE RADAR DETECTION CHARACTERISTICS OF A      *
C *      STEADY TARGET IN WEIBULL CLUTTER              *
C *
C *
C *
C *
C *
C *      Leon C. Rountree
C *
C *****
C *
C * This program was developed in order to generate data *
C * to be used to plot the probability of detection versus *
C * the signal-to-clutter ratio and the probability of    *
C * detection versus the detection range for various     *
C * values of probability of false alarm and Weibull    *
C * skewness parameters.
C *
C *****
C double precision scr,pfa,bw,alpha,beta,lna,lnb,a,b,pd,di,
+      stori,x,range
C real y,arg
C integer i,j,angle
C
C * The Weibull skewness parameter (bw) the probability of *
C * false alarm (pfa) and whether the grazing angle is    *
C * large or small (angle) is input.
C
C print *, 'ENTER THE WEIBULL SKEWNESS PARAMETER'
C read *, bw
C print *, 'ENTER THE PROBABILITY OF FALSE ALARM'
C read *, pfa
100 print *, 'ENTER A : IF THE GRAZING ANGLE IS LARGE'
C print *, '(beamwidth-limited case)'
C print *, 'ENTER A 2 IF THE GRAZING ANGLE IS SMALL'
C print *, '(pulse-length-limited case)'
C read *, angle
C if (angle .ne. 1 .and. angle .ne. 2) then
C   print *, 'INVALID DATA'
C   go to 100
C end if
C
C * The peak signal-to-noise ratio (scr) is initialized *
C * according to the value of pfa and bw. scr is in dB. *
C
C if (bw .ge. 2.d0) then

```

```

    if (pfa .ge. 1d-7) scr = 0.d0
    if (pfa .lt. 1d-7) scr = 8.d0
end if
if (bw .ge. 1.8d0 .and. bw .lt. 2.d0) then
    if (pfa .ge. 1.d-7) scr = 0.d0
    if (pfa .ge. 1.d-11 .and. pfa .lt. 1d-7) scr = 10.d0
    if (pfa .lt. 1.d-11) scr = 14.d0
end if
if (bw .ge. 1.6d0 .and. bw .lt. 1.8d0) then
    if (pfa .ge. 1.d-5) scr = 0.d0
    if (pfa .ge. 1.d-9 .and. pfa .lt. 1.d-5) scr = 12.d0
    if (pfa .lt. 1.d-9) scr = 17.d0
end if
if (bw .ge. 1.4d0 .and. bw .lt. 1.6d0) then
    if (pfa .ge. 1.d-4) scr = 0.d0
    if (pfa .ge. 1.d-7 .and. pfa .lt. 1.d-4) scr = 14.d0
    if (pfa .ge. 1.d-10 .and. pfa .lt. 1.d-7) scr = 19.d0
    if (pfa .lt. 1.d-10) scr = 22.d0
end if
if (bw .ge. 1.2d0 .and. bw .lt. 1.4d0) then
    if (pfa .ge. 1.d-3) scr = 0.d0
    if (pfa .ge. 1.d-6 .and. pfa .lt. 1.d-3) scr = 17.d0
    if (pfa .ge. 1.d-9 .and. pfa .lt. 1.d-6) scr = 23.d0
    if (pfa .ge. 1.d-12 .and. pfa .lt. 1.d-9) scr = 26.d0
    if (pfa .lt. 1.d-12) scr = 28.d0
end if
if (bw .ge. 1.d0 .and. bw .lt. 1.2d0) then
    if (pfa .ge. 1.d-2) scr = 0.d0
    if (pfa .ge. 1.d-4 .and. pfa .lt. 1.d-2) scr = 20.d0
    if (pfa .ge. 1.d-6 .and. pfa .lt. 1.d-4) scr = 25.d0
    if (pfa .ge. 1.d-8 .and. pfa .lt. 1.d-6) scr = 29.d0
    if (pfa .ge. 1.d-11 .and. pfa .lt. 1.d-8) scr = 32.d0
    if (pfa .ge. 1.d-13 .and. pfa .lt. 1.d-11) scr = 34.d0
    if (pfa .lt. 1.d-13) scr = 35.d0
end if
if (bw .ge. .8d0 .and. bw .lt. 1.d0) then
    if (pfa .ge. 1.d-2) scr = 8.d0
    if (pfa .ge. 1.d-4 .and. pfa .lt. 1.d-2) scr = 27.d0
    if (pfa .ge. 1.d-6 .and. pfa .lt. 1.d-4) scr = 33.d0
    if (pfa .ge. 1.d-8 .and. pfa .lt. 1.d-6) scr = 37.d0
    if (pfa .ge. 1.d-9 .and. pfa .lt. 1.d-8) scr = 40.d0
    if (pfa .ge. 1.d-10 .and. pfa .lt. 1.d-9) scr = 41.d0
    if (pfa .ge. 1.d-11 .and. pfa .lt. 1.d-10) scr = 42.d0
    if (pfa .ge. 1.d-12 .and. pfa .lt. 1.d-11) scr = 43.d0
    if (pfa .ge. 1.d-13 .and. pfa .lt. 1.d-12) scr = 44.d0
    if (pfa .lt. 1.d-13) scr = 45.d0
end if
if (bw .ge. .6d0 .and. bw .lt. .8d0) then
    if (pfa .ge. 1.d-1) scr = 19.d0
    if (pfa .ge. 1.d-2 .and. pfa .lt. 1.d-1) scr = 31.d0
    if (pfa .ge. 1.d-3 .and. pfa .lt. 1.d-2) scr = 37.d0

```

```

        if (pfa .ge. 1.d-4 .and. pfa .lt. 1.d-3) scr = 41.d0
        if (pfa .ge. 1.d-5 .and. pfa .lt. 1.d-4) scr = 44.d0
        if (pfa .ge. 1.d-6 .and. pfa .lt. 1.d-5) scr = 47.d0
        if (pfa .ge. 1.d-7 .and. pfa .lt. 1.d-6) scr = 50.d0
        if (pfa .ge. 1.d-8 .and. pfa .lt. 1.d-7) scr = 52.d0
        if (pfa .ge. 1.d-9 .and. pfa .lt. 1.d-8) scr = 53.5d0
        if (pfa .lt. 1.d-9) scr = 55.d0
    end if
    if (bw .lt. .6d0) then
        if (pfa .ge. 1.d-1) scr = 22.d0
        if (pfa .ge. 1.d-2 .and. pfa .lt. 1.d-1) scr = 35.d0
        if (pfa .ge. 1.d-3 .and. pfa .lt. 1.d-2) scr = 45.d0
        if (pfa .ge. 1.d-4 .and. pfa .lt. 1.d-3) scr = 50.d0
        if (pfa .ge. 1.d-5 .and. pfa .lt. 1.d-4) scr = 54.d0
        if (pfa .ge. 1.d-6 .and. pfa .lt. 1.d-5) scr = 57.5d0
        if (pfa .ge. 1.d-7 .and. pfa .lt. 1.d-6) scr = 60.2d0
        if (pfa .ge. 1.d-8 .and. pfa .lt. 1.d-7) scr = 62.5d0
        if (pfa .ge. 1.d-9 .and. pfa .lt. 1.d-8) scr = 64.6d0
        if (pfa .lt. 1.d-9) scr = 66.4d0
    end if

C
C  * Begin loop to determine the probability of detection (pd) *
C  * for current value of scr. *
C
    do 30 j = 1,10000
C
C  * Convert scr from dB value *
C
        scr = 10.d0**(scr/10.d0)
C
C  * Compute the arguments of Marcum's Q function (alpha and beta) *
C  * from equation 19. *
C
        alpha = (scr)**(1.d0/2.d0)
        beta = (2 * dlog(1.d0/pfa))**(1.d0/bw)
C
C  * The probability of detection is the Q function evaluated at *
C  * these values of alpha and beta. Compute the initial value *
C  * of pd according to equations 62 through 66 *
C
        lna = -(alpha**2.d0)/2.d0
        ln b = -(beta**2.d0)/2.d0
        a = dexp(lna)
        b = dexp(lnb)
        pd = a * b
C
C  * Begin loop to determine pd according to the recursive *
C  * relationship given by equation 61. *
C
        do 10 i = 1,2147483646
C

```

```

C      * di is a double precision value of the integer i *
C
C          di = i
C
C      * stor1 stores the previous value of pd *
C
C          stor1 = pd
C
C      * pd is determined according to equations 67 through 71 *
C
C          lna = lna + dlog((alpha**2.d0)/2.d0) - dlog(di)
C          lnb = lnb + dlog((beta**2.d0)/2.d0) - dlog(di)
C          a = dexp(lna)
C          b = b + dexp(lnb)
C          pd = pd + a * b
C
C      * If the current and previous values of pd satisfy equation 72, *
C      * then exit loop. *
C
C          if (pd.gt.1d-350.and.stor1/pd.gt..999999) go to 20
10      continue
C
C      * Convert the peak signal-to-noise ratio (scr) to the *
C      * signal-to-clutter ratio (scr) according to equation 28. *
C      * arg represents the argument of the gamma function. The *
C      * gamma function is evaluated using the INSL library. *
C      * The result of the gamma function is stored as x. *
C
C          20      arg = 1. + 2./bw
C                  x = gamma(arg)
C                  scr = (scr/2.d0)/(x**((bw/2.d0))
C
C      * For small grazing angles, the range (range) is computed *
C      * according to equation 39. *
C
C          if (angle .eq. 2) then
C              range = 1.d0/scr
C          else
C
C      * For large grazing angles, the range is computed *
C      * according to equation 38. *
C
C          range = (scr)**(-1.d0/2.d0)
C          end if
C
C      * Convert range and scr to dB. *
C
C          range = 10 * dlog10(range)
C          scr = 10.d0 * dlog10(scr)
C
C      * pd will be the y-axis in the plots of the detection *

```



```

C * characteristics. To obtain plots similar to those *
C * produced in radar literature, the y-axis was *
C * adjusted as follows: *
C
      if (pd .gt. .0001 .and. pd .lt. .9999) then
        if (pd .le. .001) y = (log10(pd) + 4.) * 8.54
        if (pd .gt. .001 .and. pd .le. .01)
+          y = (log10(pd) + 3.) * (18.87 - 8.54) + 8.54
        if (pd .gt. .01 .and. pd .le. .1)
+          y = (log10(pd) + 2.) * (32.82 - 18.87) + 18.87
        if (pd .gt. .1 .and. pd .le. .2)
+          y = (log10(pd)+1.)*(1./log10(2.))*(38.87-32.82)+32.82
        if (pd .gt. .2 .and. pd .le. .3)
+          y = 10. * (pd - .2) * (43.23 - 38.87) + 38.87
        if (pd .gt. .3 .and. pd .le. .7)
+          y = (5./2.) * (pd - .3) * (56.94 - 43.23) + 43.23
        if (pd .gt. .7 .and. pd .le. .8)
+          y = 10. * (pd - .7) * (61.13 - 56.94) + 56.94
        if (pd .gt. .8 .and. pd .le. .9)
+          y = (log10(1.-pd)+1.)*(1./log10(2.))*(61.13-67.26)+67.26
        if (pd .gt. .9 .and. pd .le. .99)
+          y = (log10(1. - pd) + 2.) * (67.26 - 81.37) + 81.37
        if (pd .gt. .99 .and. pd .le. .999)
+          y = (log10(1. - pd) + 3.) * (81.37 - 91.53) + 91.53
        if (pd .gt. .999)
+          y = (log10(1. - pd) + 4.) * (91.53 - 100.) + 100.
C
C * If pd is between .0001 and .9999, output scr, range, pd, and y *
C * which can be used to develop plots. *
C
      print '(f10.4,f10.4,f10.6,f10.4)', scr, range, pd, y
      end if
C
C * Stop when pd is greater than .9999 *
C
      if (pd .gt. .9999) stop
C
C * Convert the signal-to-clutter ratio (scr) back to the *
C * peak signal-to-noise ratio (scr). *
C
      scr = 10.d0**(scr/10.d0)
      scr = scr * 2.d0 * x**(bw/2.d0)
      scr = 10.d0 * dlog10(scr)
C
C * Increment scr. *
C
      scr = scr + .01
C
C * Repeat calculations. *
C
30 continue

```

end

Appendix B. Weibull Probability Density Function

The Weibull pdf described by equation 7 has two parameters, α and b . The parameter α is related to the median of the Weibull distribution, w_m , by equation 8, while b determines the skewness of the distribution. Figure 31 is a plot of the Weibull pdf for several values of b with $w_m = 1$.

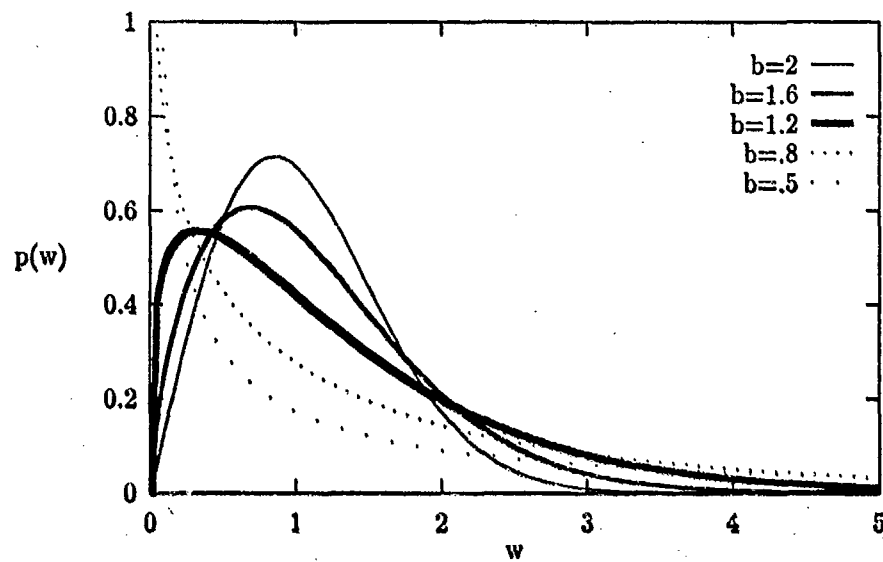


Figure 31. Weibull pdf

Bibliography

1. Boothe, Robert R. *The Weibull Distribution Applied to the Ground Backscatter Coefficient*. 12 June 1969. U.S. Army Missile Command Report RE-TR-69-15 (AD-691109).
2. Bussgang, J.J. and others. "A Unified Analysis of Range Performance of CW, Pulse, and Pulse Doppler Radar," *Radar Range Equation*, volume 2, edited by D.K. Barton, Dedham, Massachusetts: Artech House, Inc., 1977.
3. Chen, Pin Wei and W.C. Morchin. "Detection of Targets in Noise and Weibull Clutter Background," *NAECON '77 Record*, 929-933.
4. Davenport, Wilbur B., Jr. *Probability and Random Processes*. New York: McGraw-Hill Book Company, 1970.
5. DiFranco, J.V. and W.L. Rubin. *Radar Detection*. Englewood Cliffs, New Jersey: Prentice-Hall, Inc., 1968.
6. Ekstrom, J.L. "The Detection of Steady Targets in Weibull Clutter," *Radar Clutter*, volume 5, edited by D.K. Barton, Dedham, Massachusetts: Artech House, Inc., 1977.
7. Fehlner, L.F. *Marcum and Swerling's Data on Target Detection by Pulsed Radar*. Report TG-451. E. Johns Hopkins University Applied Physics Laboratory, Silver Springs, Maryland, 2 July 1962 (AD-602-121).
8. Fray, Capt. Richard P. *Simulation of Chaff Cloud Signature*. M.S. thesis, AFIT/GE/ENG/85D-16. School of Engineering, Air Force Institute of Technology (AU), Wright-Patterson AFB OH, December 1985 (A164106).
9. Goldstein, G.B. "False-Alarm Regulation in Log-Normal and Weibull Clutter," *IEEE Transactions AES*, 9: 84-92, January 1973.
10. *The ISML Library Reference Manual* (edition 9). Houston, Texas: IMSL, Inc., 1982.
11. James, M.L. and others. *Applied Numerical Methods for Digital Computation*. New York: Harper and Row, Publishers, 1985.
12. Marcum, J.I. and P. Swerling. "A Statistical Theory of Target Detection by Pulsed Radar," *IRE Transactions IT*, 6: 59-308, April 1960.
13. Melsa, James L. and David L. Cohn. *Decision and Estimation Theory*. New York: McGraw-Hill Book Company, 1982.
14. Meyer, Daniel P. and Herbert A. Mayer. *Radar Target Detection Handbook of Theory and Practice*. New York: Academic Press, Inc., 1973.

15. Minkler, G. and J. Minkler. *The Principles of Automatic Radar Detection in Clutter CFAR*. Baltimore: Magellan Book Company, 1990.
16. Nathanson, Fred E. *Radar Design Principles*. New York: McGraw-Hill Book Company, 1969.
17. Pyati, Vittal. Class handout distributed in EENG 666, Detection and Estimation Theory. School of Engineering, Air Force Institute of Technology (AU), Wright-Patterson AFB OH, April 1990.
18. Schleher, D.C. "Radar Detection in Weibull Clutter," *IEEE Transactions AES*, 12: 736-743, November 1976.
19. Skolnik, Merrill I. *Introduction to Radar Systems*. (second edition) New York: McGraw-Hill Book Company, 1980.

Vita

Leon C. Rountree was born 24 August 1963 in Macon, Georgia. He graduated from high school in Macon, Georgia in 1981. He then began a dual degree program from which he received a Bachelor of Science degree from the University of Georgia and a Bachelor of Electrical Engineering degree from the Georgia Institute of Technology. Upon graduation in September 1986, he was employed by the Warner Robins Air Logistics Center, Robins AFB, Georgia, as an avionics test engineer. He entered the School of Engineering at the Air Force Institute of Technology in June 1989.

Permanent address: WR-ALC/MAITBA
Robins AFB, Georgia 31098

REPORT DOCUMENTATION PAGE			Form Approved OMB No. 0704-0188	
Public reporting burden for this collection of information is estimated to average 1 hour per response, including the time for reviewing instructions, searching existing data sources, gathering and maintaining the data needed, and completing and reviewing the collection of information. Send comments regarding this burden estimate or any other aspect of this collection of information, including suggestions for reducing this burden, to Washington Headquarters Services, Directorate for Information Operations and Reports, 1215 Jefferson Davis Highway, Suite 1204 Arlington, VA 22202-4302, and to the Office of Management and Budget, Paperwork Reduction Project (0704-0188), Washington DC 20503.				
1. AGENCY USE ONLY (Leave blank)	2. REPORT DATE 1 November 1990	3. REPORT TYPE AND DATES COVERED M.S. Thesis (Jan 90 - Nov 90)		
4. TITLE AND SUBTITLE THE RADAR RANGE EQUATION FOR THE DETECTION OF STEADY TARGETS IN WEIBULL CLUTTER		5. FUNDING NUMBERS		
6. AUTHOR(S) Leon C. Rountree, BS, BEE				
7. PERFORMING ORGANIZATION NAME(S) AND ADDRESS(ES) AFIT/ENG Air Force Institute of Technology School of Engineering Wright-Patterson AFB, OH 45433		8. PERFORMING ORGANIZATION REPORT NUMBER AFIT/GE/ENG/90D-53		
9. SPONSORING/MONITORING AGENCY NAME(S) AND ADDRESS(ES)		10. SPONSORING/MONITORING AGENCY REPORT NUMBER		
11. SUPPLEMENTARY NOTES Thesis Chairman: Dr. Vittal Pyati				
12a. DISTRIBUTION/AVAILABILITY STATEMENT Approved for Public Release; Distribution Unlimited see b fa			12b. DISTRIBUTION CODE	
13. ABSTRACT (Maximum 200 words) In this thesis, the detection characteristics of a steady target immersed in radar clutter characterized by returns statistically modeled according to a Weibull probability density function are developed. A detector model is developed by modifying an envelope detection scheme used to detect deterministic signals in Gaussian noise. By examining the statistics of the detector output under alternate hypotheses, an expression for the probability of detection (P_d) is developed in terms of the probability of false alarm (P_{fa}), the signal-to-clutter ratio (SCR), and the Weibull skewness parameter (b), which is a function of the type of terrain causing the clutter. This expression is used in conjunction with a form of the radar range equation for area clutter to describe the relationship between P_d , P_{fa} , SCR, b , and the radar detection range. This relationship involves Marcum's Q function and an algorithm is presented which evaluates this function. The algorithm is a series approximation, also presented as a recursive relationship, that can be computed to a desired precision. Plots of P_d versus SCR and P_d versus range are developed for various values of P_{fa} and b . The plots provide a means of evaluating the detector performance and predicting the radar detection range for several values of b . <i>Keywords: Thesis</i>				
14. SUBJECT TERMS Radar Detection, Radar Clutter, Radar Range Equation, Weibull Probability Density Function, <i>INDEX</i>			15. NUMBER OF PAGES 76	
17. SECURITY CLASSIFICATION OF REPORT Unclassified			16. PRICE CODE	
18. SECURITY CLASSIFICATION OF THIS PAGE Unclassified		19. SECURITY CLASSIFICATION OF ABSTRACT Unclassified		20. LIMITATION OF ABSTRACT Unlimited